THE AMERICAN MINERALOGIST
JOURNAL OF THE MINERALOGICAL SOCIETY OF AMERICA

Vol. 31 JANUARY-FEBRUARY, 1946 Nos. 1 and 2

CHROME MICAS

D. R. E. WHITMORE,[1] L. G. BERRY AND J. E. HAWLEY,
Queen's University, Kingston, Ontario.

ABSTRACT

Some optical, chemical and x-ray studies have been made on several chromium micas (fuchsite and mariposite) of the type associated with many pre-Cambrian gold deposits.

A study of available analyses of fuchsite, including a new one by Whitmore yields the following chemical formula:

$$(K,Na,Ca)_{3.64}(Al,Mg,Cr,Fe''',Fe'')_{7.92}(Al_4,Si_{12})O_{38.61}(OH)_{9.39},$$

which closely approaches the accepted muscovite formula, $K_4Al_8(Al,Si_3)_4O_{40}(OH)_8$, representing the ideal unit cell content. In fuchsite Cr replaces Al up to 4.81% Cr_2O_3, corresponding closely to 1 atom of chromium per unit cell. Optical properties of fuchsite show the following variation: $\alpha = 1.559$ to 1.569, $\beta = 1.593$ to 1.604, $\gamma = 1.597$ to 1.611; 2V 30°–46°, indices increasing with increase in chromium. X-ray studies confirm the structural identity of fuchsite with muscovite. The varietal name *chromian muscovite* is preferred to the name *fuchsite*.

Available analyses of mariposite show a decidedly lower content of Cr_2O_3 and Al_2O_3 and higher SiO_2. The highest observed chromium content is 0.78% Cr_2O_3. The aluminum-silicon ratio in tetrahedral groups is between 2:14 and 1:15, compared with a ratio of 4:12 in fuchsite and muscovite. Published optical data show mariposite with higher indices than fuchsite and 2V 0°–14°. X-ray studies have not yet established the structural type of mica to which it belongs, but it is tentatively classed as chromian phengite.

Consideration is given to the association of these micas with hydrothermal carbonate zones and quartz-sulfide gold deposits.

INTRODUCTION

Chrome micas, classed variously as fuchsite, mariposite, and chromiferous muscovite are of wide distribution throughout gold-bearing districts of the Canadian Shield and have been noted in many other areas throughout the world. Because of their rather intimate association with ferruginous carbonate alteration zones and auriferous quartz veins, particularly in Canada, adjoining what have been recognized in recent years as prominent faults, a detailed investigation of this series of micas appears amply warranted.

[1] Part of this investigation was carried out by D. R. E. Whitmore aided by a bursary from the National Research Council, Canada, 1940.

Problems related to these brilliant green minerals are of two types. Mineralogically there is the question of their exact identity and place in the mica family, and their variations chemically and optically. Geologically it is of interest to inquire into the conditions of their formation and their source and place in the sequence of ore and gangue minerals with which they are associated.

Character of Investigation and Acknowledgments

The present investigation has included *x*-ray, chemical and optical studies of chromiferous micas. To Dr. Charles Palache of Harvard University the writers are greatly indebted for an excellent set of museum specimens representative of occurrences in California, Maine, Vermont, Quebec, Ontario, Manitoba, India, Russia, Silesia and the Tyrol. Grateful acknowledgment is also made to H. S. Spence, Mines Branch, Department of Mines and Resources, Ottawa, for an excellent specimen of fuchsite schist from Pointe du Bois, Manitoba, from which a pure concentrate was obtained of fuchsite which has been analyzed by Whitmore. In addition many other specimens from Porcupine and Larder Lake districts of Ontario have been examined and a thin-section study made of some from mines in these areas.

Due to the exceptionally fine-grained character of fuchsite and mariposite in most Canadian samples and our inability to secure pure concentrates from these, several chemical studies planned were not completed. Lack also of good crystals or fragments of mariposite have prevented any *x*-ray study of this mineral being made. There is obvious need for additional analyses and *x*-ray study when coarser-grained material is available.

X-ray studies were carried out with a Cu-target tube and Weissenberg *x*-ray goniometer.

Concentration of samples for analyses was effected both by careful crushing and screening—to remove ankerite—and by the use of Thoulet solution diluted to give specific gravities just above and below recorded gravities of fuchsite, 2.88 and 2.82 respectively.

The chemical analysis on Pointe du Bois fuchsite, by Whitmore, employed Washington's (1930) standard procedure for the determination of SiO_2, Fe_2O_3, Al_2O_3, CaO, Na_2O and K_2O. TiO_2 was determined gravimetrically using cupferron because of the considerable quantity present. MgO was determined by a method described by Fales (1925), while chromium was determined colorimetrically according to a method described by Groves (1937).

Minor constituents present in four fuchsites and in a number of ore and gangue minerals associated with chrome mica in specimens from the

Hollinger mine were determined using a Hilger E 316 spectrograph and copper electrodes. Optical studies were carried out with monochromatic light, in some cases using the double variation method of Emmons, and optic angles were measured on a Zeiss universal stage. The limit of accuracy of index determination was found to vary greatly with increasing fineness of the mica flakes, and for very fine-grained material may be as much as $\pm .005$.

Review of the Literature

A bibliography on chrome micas is appended to this paper. Here only the more important references need be mentioned in order to show some of the ideas held with regard to their nomenclature. In many cases analyses are given without any or adequate optical data, in others the latter are available for unanalyzed material. In much of the Canadian literature the mica is named without adequate chemical or optical data to support it.

Fuchsite

The original fuchsite, named after the chemist J. H. von Fuchs, is from Schwarzenstein in the Zillerthal. An analysis by Schafhautl, appearing in Dana (1882), shows over 5 per cent Cr_2O_3. Five other analyses of chrome micas from Belgium, Maryland, Aird Island, L. Huron; Sysersk, Urals and Ouro Preto, are recorded in Dana (1892), the first four of which have been used in this work. Others have appeared since by Prior (1908), Partridge (1937) and Hutton (1940 and 1942).

The Cr_2O_3 content of these ranges from 0.84 to 3.95 per cent. Wherry (1916), notes that a fuchsite from Marble, Colorado, contains 6.08 per cent Cr_2O_3, the highest chromium content on record, but no optical data are given.

Optical studies include those by Szadeczky-Kardoss (1937) and by Partridge and Hutton on analysed material. Szadeczky-Kardoss concluded that fuchsite is a first grade mica, that the optical properties vary with depth of colour and hence, presumably with the chromium content, and that both refractive indices and birefringence increase with increasing colour.

The only *x*-ray study of chrome-mica is one by Pauling (1930) made casually on fuchsite (as a variety of muscovite), by oscillation and Laue photographs.

Partridge (1936) reporting on chrome-mica from South Africa prefers the term *chrome-muscovite* to *fuchsite*. Odman (1938) favours *mariposite* for a low Cr-mica, despite the fact that his material is identical optically

with low Cr-fuchsites. Again, in 1940, Hutton suggests the term *mariposite* be abandoned (apparently only on the basis of its low Cr content) and recommends the term *chromiferous muscovite* for those containing 1 per cent Cr_2O_3 and *fuchsite* for those with more. There is thus very obvious need of a clear statement of the characteristics of these minerals.

Mariposite

The type locality for mariposite is the Mariposa estate, in the southern part of the Mother lode district in California, described by Silliman (1868) and Turner (1895), and later by Knopf (1929). Analyses of this material by Hillebrand (1900, in Turner, 1895) include a white non-chromium-bearing mica and a green mariposite with 0.18 per cent Cr_2O_3. In these, as in alurgite, a manganiferous mica, as noted by Schaller[2] (1916), a high SiO_2:Al_2O_3 ratio is characteristic. Winchell (1925) using Hillebrand's analysis relates mariposite to high silica phengite and protolithionite and considers the continuity of the series of heptaphylite micas from muscovite to mariposite as established, in which case the chromium content is merely incidental. Later Winchell (1927) modifies his concept of the phengite molecule which is again revised by Volk (1939), but for muscovites *not* as siliceous as those used by Winchell.

Only one other analysis of mariposite by Moorehouse, described by Moore (1936) appears in the literature. Optical data is confined to that given by Knopf (1929) and Moorehouse.

In considering the relation of the chrome micas to the family to which they belong reference must be made to the work of Berman (1937), and Hendricks and Jefferson (1939), whose concepts of the structure of the micas have been followed in this paper.

Important papers dealing with the origin of chromiferous micas are those of Cooke (1922) and Partridge (1937) while many other descriptions of occurrences both in Canada and elsewhere give pertinent data in this respect.

Results of Investigation

X-ray Study

The first and fundamental problem was to confirm the structural identity of fuchsite with muscovite by *x*-ray analyses which were carried out by L. G. Berry.

[2] A correction in Schaller's quotation of the original analysis of alurgite (Penfield, 1893) should be noted, since Mn_2O_3 content appears as Cr_2O_3.

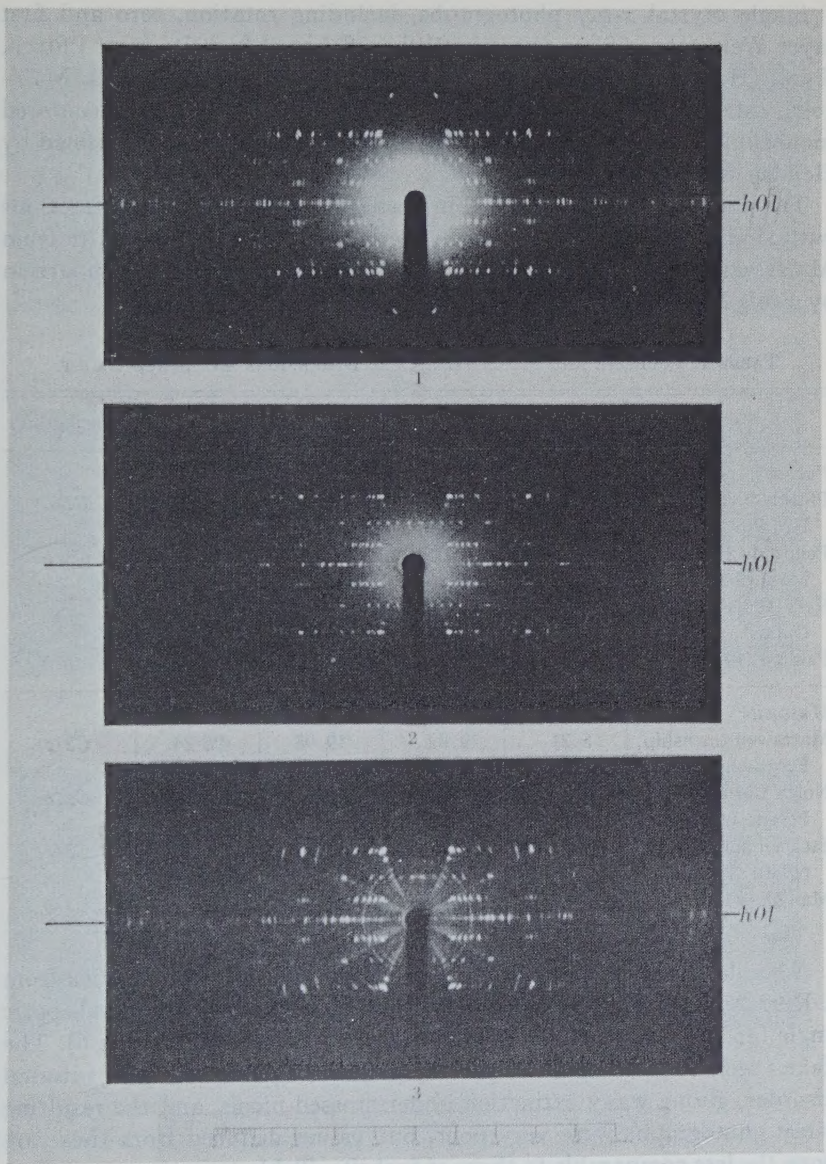

FIGS. 1–3.—Rotation photographs [010], with unfiltered Cu-radiation, the scale gives millimetres on the film or degrees of θ. Fig. 1.—Muscovite, lot 6, concession II, Mattawan township, Nipissing District, Ontario (photograph by Ferguson (1943). Fig. 2.—Fuchsite, Pfitsch, Tyrol, HM 90948. Fig. 3.—Fuchsite, Pointe du Bois, Manitoba.

Single crystal x-ray photographs, including rotation, zero and first layer Weissenberg films about b [010] on flakes of fuchsite from Pfitsch, Tyrol (Harvard Museum Specimen 90948), and Pointe du Bois, Manitoba, establish these as belonging to the same two-layer, base-centered monoclinic mica structure, characteristic of muscovite as determined by Hendricks (1939).

The photographs are identical in position and intensity of diffractions with similar photographs taken by Ferguson (1943) of muscovite from Mattawan township, Ontario, which were kindly loaned for comparison by Prof. M. A. Peacock, University of Toronto (Figs. 1 to 9).

TABLE 1. FUCHSITE AND MUSCOVITE: CELL DIMENSIONS AND SPACE GROUP

	a	b	c	β	Space group
Fuchsite					
Pfitsch, Tyrol HM 90948	5.19 Å	8.99 Å	19.98 Å	95°52′	$C2/c$
Pointe du Bois, Manitoba	5.19	9.03	19.97	95 00	$C2/c$
Kerr Addison Mine, Ontario	5.2	8.97	19.98	95 30	—
Pauling (1930)	5.19	8.99	20.14	96	—
Muscovite					
Mattawan township, Ferguson (1943)	5.21	9.02	19.98	96 24	$C2/c$
North Carolina, Ferguson (1943)	5.20	9.03	20.04	95 54	$C2/c$
Jackson and West (1930)	5.18	9.02	20.04	95 30	$C2/c$
Mauguin (1927)	5.17	8.94	20.01	96	$C2/c$

A similar series of photographs were taken of a flake of Cr-mica from a Kerr Addison mine specimen, which peculiarly showed a small optic angle (15°–20°) but indices close to those of fuchsite (see Table 6). The flake used consisted of a sub-parallel growth or possessed some internal disorder, giving wavy extinction under crossed-nicols, and the resulting x-ray photographs were very poor, but values deduced from these are none the less comparable to those of fuchsite. Table 1 gives a comparison of the cell dimensions of the above micas with the previous determination by Pauling and with other determinations on muscovite by Ferguson (1943), Jackson and West (1930) and Mauguin (1927). All are in good agreement.

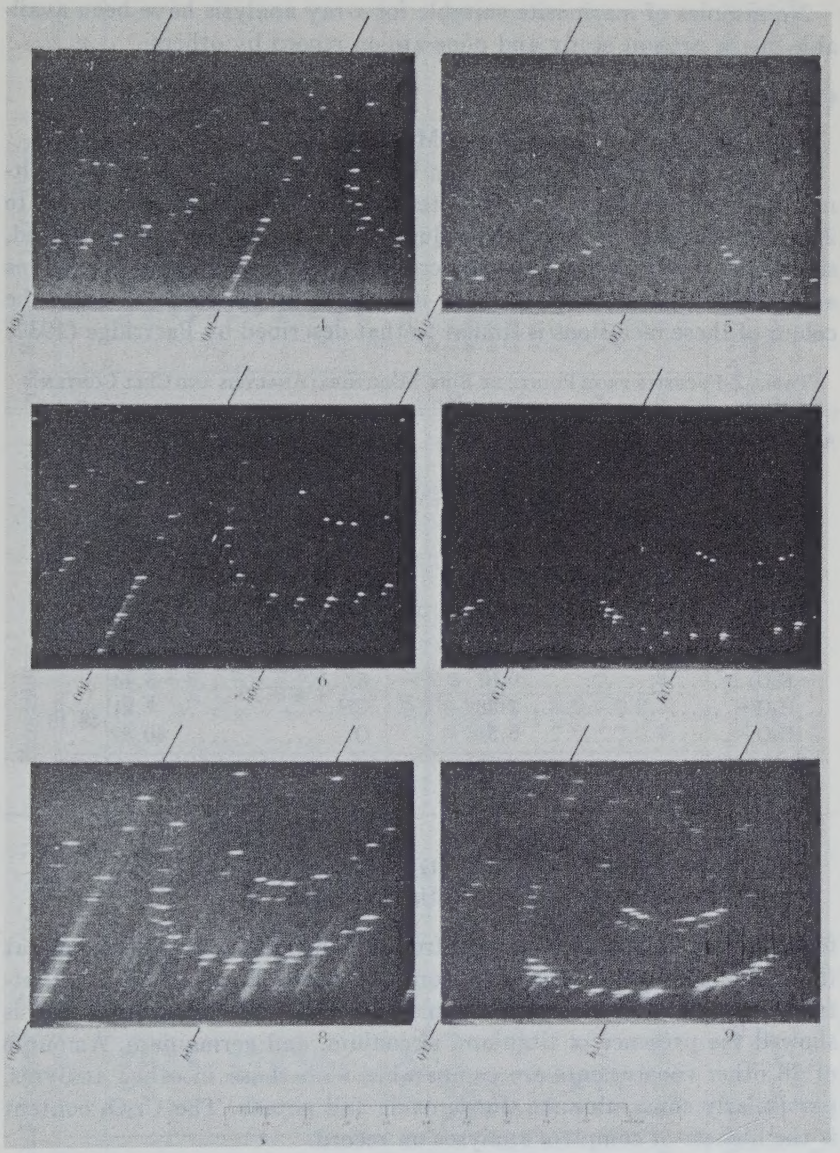

FIGS. 4, 6, 8.—Weissenberg resolution of the zero layer line (*h*0*l*). FIGS. 5, 7, 9.—Weissenberg resolution of the first layer line (*h*1*l*), all with unfiltered Cu-radiation, same scale as Figs. 1–3. Figs. 4, 5.—Muscovite, lot 6, concession II, Mattawan township, Nipissing District, Ontario (photograph by Ferguson (1943). Figs. 6, 7.—Fuchsite, Pfitsch, Tyrol, HM 90948. FIGS. 8, 9.—Fuchsite, Pointe du Bois, Manitoba.

No samples of mariposite suitable for x-ray analysis have been available in the present study and none are on record by others.

Chemical Composition

Fuchsite from Pointe du Boise, Manitoba.

The new analysis of fuchsite from Pointe du Bois, Manitoba, by Whitmore, is given in Table 2. TiO_2 determined on the sample amounted to 2.23 per cent, which has been deducted and the analysis recalculated, since most if not all of it is to be accounted for by abundant fine prisms and twins of a golden brown rutile intergrown in the fuchsite. Since the colour of these inclusions is similar to that described by Partridge (1937)

Table 2. Fuchsite from Pointe du Bois, Manitoba: Analysis and Cell Content

Analysis (Whitmore)		Cell content with $M=1628$		
SiO_2	45.97	Si	12.45	16.00
Al_2O_3	31.67	Al	10.10	
Fe_2O_3	2.56	Fe'''	0.52	
Cr_2O_3	4.81	Cr	1.03	8.34
FeO	0.53	Fe''	0.12	
MgO	0.31	Mg	0.12	
CaO	0.15	Ca	0.04	
Na_2O	1.03	Na	0.54	3.72
K_2O	9.07	K	3.14	
H_2O+	3.48	OH	7.21	48.10
H_2O-	0.51	O	40.89	
	100.09			

Structural formula:
$4[(K, Na, Ca)_{0.93}(Al, Cr, Fe''', Fe'', Mg)_{2.08}(Al_{0.89}Si_{3.11})O_{10.22}(OH)_{1.80}]$
Ideal formula of muscovite: $4[KAl_2(AlSi_3)O_{10}(OH, F)_2]$

for chromiferous rutile in fuchsite from Mashishimala, it is possible that this rutile also contains some chromium in which case total Cr_2O_3 attributed to the mica may be somewhat high. Spectroscopic analysis showed the presence of titanium, zirconium, and germanium. Amounts of all other constituents are comparable with those in other analyses, particularly silica, alumina, ferric oxide and potash. The Cr_2O_3 content is the highest of complete analyses on record.

The cell dimensions of this fuchsite, combined with the measured specific gravity, 2.88, give the cell content in Table 2, and the structural formula. This compares closely with the ideal formula of muscovite, with Cr taking the place of Al to the amount of 1 atom. The ratio of Al:Si in tetrahedral coordination is close to 1:3, and the total number of oxygen and hydroxyl ions is clearly 48.

TABLE 3. FUCHSITE: ANALYSES AND ANALYSES REDUCED TO ATOMIC PROPORTIONS ON THE BASIS OF O=48 ATOMS

	1	2	3	4	5	6	7	8	9	10
SiO_2	44.87	45.68	43.51	47.24	42.21	45.49	46.17	46.35	45.97	
Al_2O_3	37.72	34.17	36.86	31.86	34.55	31.08	29.71	29.69	31.67	
Fe_2O_3	0.54	2.35	2.05	—	1.03	tr.	2.03	0.23	2.56	
Cr_2O_3	0.27	0.84	0.85	0.87	2.03	3.09	3.51	4.60	4.81	
FeO	nil	—	—	0.56	—	—	—	0.85	0.53	
MgO	0.32	3.84	1.02	2.91	3.13	3.36	2.28	1.93	0.31	
CaO	0.36	0.27	0.55	0.58	0.47	0.51	—	tr.	0.15	
Na_2O	1.04	2.23	1.34	0.16	0.82	0.90	—	0.78	1.03	
K_2O	9.83	4.47	8.11	10.72	9.16	9.76	10.40	10.53	9.07	
H_2O+	4.72	4.65	5.80	5.37	6.77	5.85	5.42	4.69	3.99	
H_2O-	0.38	—	—	—	—	—	—	0.12	—	
F	nil	—	—	—	—	—	—	0.04	—	
	100.24[1]	98.50[3]	100.55[4]	100.41[5]	100.17	100.04	99.52	100.31[7]	100.09	
Si	11.76 } 16.00	12.05 } 16.00	11.40 } 16.00	12.42 } 16.00	11.02 } 16.00	12.00 } 16.00	12.35 } 16.00	12.45 } 16.00	12.43 } 16.00	12.00 } 16.00
Al	11.65	10.62	11.38	9.86	10.62	9.65	9.35	9.40	10.09	
Fe'''	0.10	0.47	0.40	—	0.20	—	0.41	0.05	0.52	
Cr	0.06 } 7.72[2]	0.17 } 8.82	0.18 } 7.76	0.18 } 7.90[6]	0.42 } 7.48	0.64 } 7.61	0.74 } 7.76	0.98 } 7.90[8]	1.03 } 8.31	} 7.92
Fe''	—	—	—	0.12	—	—	—	0.19	0.12	
Mg	0.13	1.51	0.40	1.17	1.22	1.32	0.91	0.77	0.12	
Ca	0.10	0.08	0.15	0.16	0.13	0.14	—	—	0.04	
Na	0.53 } 3.92	1.14 } 2.72	0.68 } 3.54	0.08 } 3.84	0.41 } 3.59	0.46 } 3.88	— } 3.54	0.41 } 4.04[9]	0.54 } 3.70	} 3.64
K	3.29	1.50	2.71	3.60	3.05	3.28	3.54	3.61	3.12	
OH	9.19	8.17	10.12	9.41	11.80	10.30	9.65	8.63	7.19	9.39
O	38.81 } 48.00	39.83 } 48.00	37.88 } 48.00	38.59 } 48.00	36.20 } 48.00	37.70 } 48.00	38.35 } 48.00	39.34 } 48.00	40.81 } 48.00	38.61 } 48.00
F	—	—	—	—	—	—	—	0.03	—	—

1. **Westland**, South Island, New Zealand; anal. Seelye (in Hutton, 1940); [1]incl. TiO_2 0.02, V_2O_3 0.09, MnO tr., Li_2O tr., P_2O_5 0.08; [2]incl. Ti 0.003, V 0.02. 2. Salm Chateau, **Belgium**; anal. Klement (1888) (in Dana, 1892); [3]incl. Li_2O tr. 3. Mashishimala, Transvaal, South Africa; anal. Partridge (1937); [4]incl. Cs_2O tr. 4. Binnenthal, Switzerland; anal. **Prior (1908)**; [5]incl. Li_2O 0.14; [6]incl. Li_2O 0.15. 5. Montgomery Co., Maryland; anal. Chatard (in Gill, 1889, in Dana, 1892). 6. Aird Islands, Lake Huron; anal. Cairns (in Chester, **1887)**. 7. Sysersk, Urals; and Damour (1882). 8. Dead Horse Creek, Lake Wakatipu region, Western Otago, New Zealand; anal. Seelye (in Hutton, 1942); [7]incl. TiO_2 0.28, MnO **0.01, BaO 0.15**, P_2O_5 0.01. V_2O_3 tr., S 0.05; [8]incl. Ti 0.06, Mn'' 0.002; [9]incl. Ba 0.02. 9. Pointe du Bois, Manitoba; anal. Whitmore. 10. Average numbers of atoms.

Comparison of Analyses

All available analyses with the exception of one from the Zillerthal (Dana) in which no water is listed, have been reduced to atomic proportions on the basis of (O, OH, F) = 48 and are presented in Table 3 for comparison. These are arranged in order of increasing Cr content which varies from 0.06 to 1.03 atoms per unit cell, the equivalent of 0.27% to 4.81% by weight. The average is given in the last column in which Si = 12.0, Al (tetrahedral coordination) = 4.0, Al, Cr, etc. (octahedral) = 7.92, K, Na, etc. = 3.64, and (OH, F) = 9.39, all agreeing well with the ideal structural formula of muscovite. Fuchsites covering this range of composition are thus established as identical with muscovite.

Chemical Composition of Mariposite

The three available analyses of mariposite by Hillebrand (Turner, 1895) and Moorehouse (Moore, 1936) are given in Table 4, as calculated in atomic proportions on the basis of (O, OH, F) = 48 atoms, and are compared with similarly calculated analyses of alurgite (Penfield, 1893) and fuchsite (Manitoba).

All mariposites show a low Cr_2O_3 content (0%–0.78% by weight) resembling in this respect some of the low-chrome-fuchsites, but this is no reason to eliminate the term mariposite, as suggested by Hutton (1940), especially since the three analyses show a consistently low Al:Si ratio compared with fuchsite. In mariposite the Al:Si ratio for atoms in tetrahedral coordination is between 2:14 and 1:15 as against 4:12 in fuchsite, and as noted previously by Winchell (1925) this feature appears characteristic of mariposite and phengite. Compared with either alurgite or the phengite molecule, Winchell (1927), mariposite is more siliceous than both and differs still more in this respect from the revision suggested for the phengite molecule by Volk (1939) who obviously dealt with muscovites of a more normal silica content.

Though the layer structure of mariposite is unknown, the analyses have been reduced to atomic proportions with (O+OH) = 48 atoms (Table 4). The average structural formula can be expressed as follows: Mariposite—

$$x[(K, Na, Ca,)_{1.68}(Al, Mg, Fe''', Fe'', Cr, Ti)_{3.96}(Al_{0.69}Si_{7.31})O_{20.3}(OH)_{3.7}].$$

This formula in which x represents the unknown number of layers may be compared with the structural formula of alurgite established as a 3-layer structure by Hendricks (1939) and with the ideal structural formula of phengite.

TABLE 4. MARIPOSITE: ANALYSES COMPARED WITH ALURGITE AND FUCHSITE, AND REDUCED TO ATOMIC PROPORTIONS ON THE BASIS OF O=48 ATOMS

	1		2		3		4		5	
SiO_2	56.79		55.35		56.00		53.22		45.97	
Al_2O_3	25.11		25.62		23.52		21.19		31.67	
Fe_2O_3	0.63		0.63		3.30		1.22		2.56	
Cr_2O_3	—		0.18		0.78		—		4.81	
Mn_2O_3	—		—		—		0.87		—	
FeO	0.92		0.92		0.51		—		0.53	
MnO	—		—		—		0.18		—	
MgO	3.29		3.25		2.12		6.02		0.31	
CaO	0.07		0.07		0.37		—		0.15	
Na_2O	0.17		0.17		2.72		0.34		1.03	
K_2O	8.92		9.29		7.03		11.20		9.07	
H_2O	4.72		4.52		3.52		5.75		3.99	
	100.80[1]		99.95[3]		99.87		99.99		100.09	
Si	14.61	16.00	14.43	16.00	14.85	16.00	14.04	16.00	12.43	16.00
Al	7.61		7.89		7.35		6.58		10.09	
Fe'''	0.12		0.12		0.66		0.24		0.52	
Cr	—		0.04		0.16		—		1.03	
Mn'''	—	7.80[2]	—	7.94[4]	—	7.97	0.17	7.43	—	8.31
Fe''	0.20		0.20		0.11		—		0.12	
Mn''	—		—		—		0.04		—	
Mg	1.26		1.26		0.84		2.36		0.12	
Ca	0.02		0.02		0.11		—		0.04	
Na	0.08	3.03	0.06	3.16	1.40	3.89	0.17	3.94	0.54	3.70
K	2.93		3.08		2.38		3.77		3.12	
OH	8.10	48.00	7.85	48.00	6.22	48.00	10.11	48.00	7.19	48.00
O	39.90		40.15		41.78		37.89		40.81	

1 and 2. Mariposite, Mariposa region, California; anal. Hillebrand (1900) (in Turner, 1895); [1]incl. TiO_2 0.18, [2]incl. Ti 0.03, [3]incl. TiO_2 0.18, [4]incl. Ti 0.03. 3. Ross Mine, Hislop township, Ontario, anal. Moorehouse (in Moore, 1936). 4. Alurgite, St. Marcel, Piedmont, Italy; anal. Penfield (1893). 5. Fuchsite Pointe du Bois, Manitoba; anal. Whitmore.

Alurgite—

$$3[(K, Na)_{1.97}(Al\ Mg, Fe''', Mn''', Mn'')_{3.71}(Al_{0.92}Si_{7.02})O_{18.96}(OH)_{5.05}];$$

Phengite—

$$2\ (?)[K_2(Al, Mg, Fe'')_4(Al, Si_7)\ O_{20}(OH, F)_4].$$

The similarity of mariposite to both alurgite and phengite is thus readily apparent. Since alurgite characteristically contains manganese, and has practically the same Al:Si ratio as phengite, it seems best to

restrict this term to manganiferous phengites, and to regard mariposite essentially as a chromiferous phengite. Further comparison must await determination of the layer structure, but in the meantime we have no reason to disagree with Winchell (1925) in his statement that "the continuity of the series from muscovite to mariposite can no longer be questioned."

Optical Properties

Fuchsite

In Table 5 the important optical properties of twelve specimens of fuchsite are arranged in order of increasing Cr_2O_3 content. Data on seven other samples, the Cr_2O_3 content of which is not known, are also included. All are optically negative, with the optic plane $\perp$ (010) as far as determined. Indices of refraction range from 1.559 for α to 1.6115 for γ. The average β for 12 analyzed specimens is 1.598.

In general the indices rise with increasing tenor of Cr_2O_3. Birefringence is very strong, 0.035–0.042, and affords a ready method of distinguishing these micas from similarly coloured chlorites. Optic angle (2V) determinations show a range from 32°–46° with an average value of 36°. Absorption formula $= X < Y < Z$; Pleochroism is noted by some authors as very distinctive, with

α = robin's egg blue
β = yellow, yellowish green
γ = blue green.

In thick flakes dispersion is distinct with $r > v$.

Examination of material from the Hollinger and McIntyre Mines, Porcupine District, Ontario, and from Plymouth, Vermont (HM 90940), shows that green micas of two types are present—one with a small optic angle, another with a larger $2V$, characteristic of fuchsite. As noted above the green mica from the Kerr Addison Mine also shows a small optic angle though x-ray analysis suggests it is similar to fuchsite. All of these micas with small $2V$ show wavy extinction and either consist of subparallel aggregates or have a somewhat disordered structure, possibly due to shearing movements. As shown in Table 6 indices of refraction are similar to those of fuchsite rather than mariposite, and it seems best to classify them as fuchsites, until such time as analyses show their true chemical character. Thus, while an appreciable optic angle (36°) is diagnostic of fuchsite, a smaller optic angle ($< 20°$) does not necessarily establish a chrome-mica as mariposite.

TABLE 5. FUCHSITE: OPTICAL PROPERTIES

No. and Locality	$\%Cr_2O_3$	2E	2V	Indices			biref.	
				α	β	γ		
1 Westland, N. Z. Hutton (1940)	0.27		46°	1.5590	1.5930	1.5973	.038	$G.=2.821$
2 Belgium Klement (1888)	0.84							$G.=2.819$
3 Mashishimala, S. A. Partridge (1937)	0.85		35°	1.563	1.596	1.598	.035	$r>v$ strong, $X<Y<Z$
4 New Consort Mine, S. A. Partridge (1937)	tr.		36°		1.596	1.600		
5 Binnenthal, Switzerland	0.87							
6 Montgomery Co., Md. Gill (1899)	2.03	68° Na 71° Li						$r>v$
7 Aird Is., L. Huron Chester (1887)	3.09							
8 Sysersk, Urals Damour (1882)	3.51	67° gr. 69° yel. 72° red.						$r>v$ $G.=2.88$
9 Zillerthal, Austria HM 11568, Whitmore	(3.95)	53°	32°		1.604	1.608	.037	
10 Zillerthal, Austria HM 90949, Hawley					1.598	1.606		
11 Otago, N. Z. Hutton (1942)	4.60		37°	1.5695	1.6040	1.6115	.042	$G.=2.88$
12 Pointe du Bois, Manitoba	4.81		36°		1.602	1.603	.038	$r>v$ $G.=2.88$
Unanalyzed materials								
13 Credo Porcupine Ontario, Whitmore		63°	38°		1.598	1.603	.039	
14 Trabau, Silesia HM 90947, Whitmore		56	34		1.595	1.601	.037	
15 Brunswick, Maine HM 11572, Whitmore	tr.	57	35		1.596	1.601	.036	
16 Plymouth, Vermont HM 90940, Whitmore		61	37		1.597	1.603	.038	
17 Pfitsch, Tyrol HM 90948, Whitmore		54	33		1.597	1.602	.035	
18 Rendek, Hungary Szad-Kardoss		59	36		1.602	1.609	.0355	$r>v$
19 Velem, Hungary Szad-Kardoss			30–38				.0357	

Mariposite

Optical data available on mariposites and determined on two new specimens are given in Table 7. One specimen from California is described by Knopf (1929) as uniaxial. That from Washington, noted by Larsen (1934), $2V=40°$, is exceptional compared with values of 12°–14° for mari-

Table 6. Uncertain Cr-Micas with Small Optic Angles but Indices of Fuchsite

Locality	Optic Angle 2V	Indices			Biref.
		α	β	γ	
1. Hollinger Mine, Ontario	v. small	1.561	1.594	1.596	.035
2. Plymouth, Vermont HM 90940	v. small	1.568	1.598	1.599	.031
3. Kerr Addison Mine, Ontario	16°–19°	1.561	1.597	1.601	.040

posites from the Rawhide and Hollinger mines. While some of the indices for mariposites overlap those of high-Cr fuchsites, they are somewhat greater than for fuchsites of comparable tenor of Cr_2O_3, and in some cases even exceed those with large amounts. Colour is described by Knopf as emerald green for some samples, apple green for others and white for one sample which lacks any Cr_2O_3. Mariposite from the Rawhide Mine (HM 86911) shows X = deep blue green, and $Y = Z$ paler green. Dispersion has not been determined. In view of the discovery that some apparent fuchsites, listed in Table 6, have also small optic angles, and since the differences in indices of refraction of fuchsites and mariposites are slight, it is apparent that the optical distinction of mariposite, particularly when very fine grained, must be made with considerable care.

Table 7. Mariposite: Optical Properties

No. and Locality	% Cr_2O_3	2V	Indices			biref.	Author
			α	β	γ		
1 Mother Lode, Cal.	nil						
2 Mother Lode, Cal.	0.18	0			1.60		Knopf (1929)
3 Mother Lode, Cal.	+test	($2E$=36°)	1.56 to 1.58		1.61 to 1.63		Knopf (1924) includes Rawhide Mine
4 Rawhide Mine, Cal. HM86911	+test	12°	1.565	1.601	1.605		Hawley
5 Ross Mine, Ont.	0.78	very small		1.624			Moorehouse in Moore (1936)
6 Washington		40°			1.63		Larsen (1934)
7 Hollinger Mines	+test	14°		1.617	1.621	.033	Whitmore

Summary

By means of x-ray, chemical, and optical studies fuchsites with a range in composition of 0.27%–4.81% Cr_2O_3 are identified as chromiferous muscovites, for which the varietal term *chromian muscovite* is preferred to *fuchsite*. Well formed flakes give an average $2V = 36°$ and an average $\beta = 1.598$. Finer grained material, either sub-parallel growths or strained crystals show smaller $2V$ ($< 20°$) but indices of other fuchsites.

Mariposite, apparently less plentiful, and less well studied, conforms, chemically with phengite and is regarded as a chromiferous variety of this mica. With one exception $2V$ is always small while indices are higher than for fuchsites of similar Cr_2O_3 content, and in some cases are even higher than for Cr_2O_3-rich fuchsites. Considerable care is thus needed in distinguishing it with certainty.

Occurrence and Origin of Chrome-Micas

Occurrence and Association

As far as can be determined, chrome-micas, much like sericite, have invariably been formed either by metasomatic processes or deposited directly with other minerals in veins. Minerals associated with them suggest they were formed under conditions ranging from moderate to fairly high temperatures and pressures, and give rise to a tentative three-fold classification, in all of which fine rutile is commonly present.

1. With ankerite, quartz, sulfides and gold.
2. With biotite and actinolite.
3. With corundum, biotite, cyanite.

Of these the first association is by far the most common, and is that which prevails in the numerous deposits throughout the Ontario and Quebec portions of the Canadian pre-Cambrian shield, as well as in the Mother Lode district of California, and in Western Australia. In the first area either fuchsite or mariposite may be present but nowhere is there record of both being found together in a single specimen, nor do descriptions of occurrence indicate any reason for the one forming in preference to the other.

Type 1. Ankerite-quartz-sulfide-gold association

The most notable occurrences of chrome-micas in Canada are in the Larder Lake and Porcupine Districts of Ontario, described by Wilson (1909), Cooke (1922) and Burrows (1915 and 1924). Others have been noted by Thomson (1935) in Lake of the Woods district, Ontario, by

Hawley (1929) in the Rainy River District, and by several authors along faults zones to the east of Larder Lake in Quebec. Other outstanding deposits of this type are in the southern part of the Mother Lode Deposit (mariposite, Knopf 1929), and in Western Australia (fuchsite, Simpson 1935).

In all of these the mica is developed in rusty weathering carbonatized and pyritized zones which replace a great variety of rocks, most of which have been previously rendered more or less schistose. In some, the chrome-mica carbonate zones appear to have suffered further shearing and in all cases quartz stock works penetrate the zones, in a highly irregular manner.

In recent years such zones have come to be regarded as marking either large fault zones or their close proximity, east and west of Kirkland Lake, Ontario, and in adjacent parts of northwestern Quebec.

Rock types so replaced consist of various schists, lavas, commonly andesitic to basaltic; tuffs and agglomerates; sediments, including conglomerate, quartzite, greywacke, and slate, and intrusives particularly siliceous quartz porphyries as in the Porcupine District, diorite porphyry, and even pegmatitic dykes as at Larder Lake and Pointe du Bois, Manitoba. Three occurrences have been noted in peridotites or serpentinized ultrabasic intrusions, namely fuchsite (?) in Deloro Twp., Ontario (Burrows, 1915), mariposite in a section of the Mother Lode deposit, California (Knopf, 1929) where its distribution is restricted to that part of the lode occurring in serpentine, and fuchsite in pyritiferous quartz cutting peridotite at L. Saganaga, Ontario (Whitmore). All descriptions are unanimous in ascribing a replacement or hydrothermal origin to the mica.

Detailed studies of the paragenesis of such deposits, as might be expected from their complex history and as detailed closely by Cooke (1922), show a somewhat variable position for chrome micas. At Larder Lake, Cooke notes that dolomite is cut by numerous fractures which are filled in many places by quartz, calcite or other carbonates, and locally with albite. Along these veins the dolomite is altered or replaced by fuchsite which gradually fades into gray dolomite away from the vein. The veins themselves where they narrow down to a hair-line are filled with fuchsite. From his studies Cooke concludes there was a progressive change in the carbonate-rich solutions, with a decrease first in Mg and Fe and later of Ca, with an increase in SiO_2, Cr, and sulfur.

Examination of gold-bearing specimens from the Hollinger and McIntyre mines by Whitmore show chrome-mica intergrown with ankerite as a fine felt. It replaces the carbonate, rounded remnants of which are left. Though pyrite in many schistose specimens appears to replace

chrome-mica as it does other schistose minerals, veinlets containing mariposite, some containing gold, some containing both minerals occur cutting quartz. Relations between gold and mariposite are conflicting and suggest overlapping or contemporaneity. In a number of instances gold occurs on small spurs jutting out from and is interrupted by veins of mariposite. In other cases veins of gold cut squarely across others of mariposite.

Specimens from the Credo Porcupine (Arcadia) Mine indicate early quartz was much fractured and replaced by a series of carbonate veinlets, and fuchsite was introduced after ferruginous carbonates but before later quartz-calcite veins which cut the mica. This suggests that Cr was being carried contemporaneously with iron and magnesium in CO_2-rich vein fluids and when deposition of iron either as carbonates or pyrite was completed, so was that of Cr.

On the other hand Moore (1936) notes that at the Ross Mine mariposite was formed at an early stage in the mineralization and is cut by stringers of quartz and ankerite and is impregnated with auriferous pyrite. At Pointe du Bois, Manitoba, Spence (1930) described mica schist as replaced by fuchsite and cut by later quartz-carbonate veins, while in the Mother Lode deposits of California Knopf indicates that the mariposite-ankerite masses are traversed by a network of veinlets of coarse, milky quartz.

That chromium was present in the hydrothermal solutions responsible for these complex replacement deposits during the deposition of many, if not most, of the minerals is supported by spectrographic examination of ore and gangue minerals from the Hollinger mine. Samples of ankerite, quartz, scheelite, chalcopyrite, gold and petzite from specimens in which no chrome-mica was visible, were tested, and all but the telluride yielded traces of chromium. Though the possibility of natural contamination cannot be denied, the results are certainly suggestive.

Type 2. Fuchsite with biotite or actinolite

This type is represented solely by three fuchsite specimens from the Zillerthal, Tyrol, HM 11568, 90949, 86918. The first consists of fine-grained, brilliant green fuchsite which forms a groundmass for randomly oriented books of biotite with a diameter of about 5 mm. The second is intergrown with both biotite and actinolite, and the third with biotite and quartz. Other specimens from the Tyrol contain fuchsite in dolomite resembling Type 1, but those with biotite or actinolite cannot but indicate somewhat higher conditions of temperature and pressure than likely existed during the development of the carbonate type. Unfortunately further information on these is not available to the writers.

It is possible that an occurrence at the Boliden Deposit, Sweden, (Ödman, 1941) belongs to this type. Here the green mica surrounds a lamprophyric dyke, in narrow zones, which become prominent as the dyke peters out. Where the dyke ends the green mica "follows on as an independent dyke for several meters."

Type 3. Fuchsite with corundum and cyanite

Two occurrences of fuchsite have been described with associated corundum and one with corundum and cyanite. Hutton (1940) describes fuchsite as bright green scales in corundum-bearing schist from Whitcombe Valley, Mikonui, Westland New Zealand. In the northeastern Transvaal, Partridge (1937) describes fuchsite from Mashishimala as surrounding rudely lenticular bodies of corundum-bearing rock in hornblendite near its contact with granite. The mica is intergrown in various to equal proportions with cyanite, rutile, ruby corundum, biotite and plagioclase. The reddish brown rutile shows spectroscopic traces of Cr. Though in neither case is a detailed paragenesis available, these associations of fuchsite suggest its formation under still higher temperature and pressure conditions than in types 1 and 2.

Genesis

As a product of hydrothermal metasomatism and possibly also as a true vein mineral, chrome mica may obviously owe some of its constituents to the original rocks which it replaces or in which it is found as vein fillings. On the other hand, keeping in mind the great variety of rock types in which it occurs, and the fact that no clear cut case of pseudomorphism, as of sericite after feldspar, has been cited, it is possible that most of its constituents and particularly the chromium, have had their origin in solutions derived from some magmatic source. Since only the chromium is at all distinctive we may consider the views held with respect to it.

Chromium derived from replaced rocks

As indicated above only three cases have been found where chrome-micas occur in ultrabasic rocks or their serpentinized equivalents. The close spatial relations of mariposite in the Mother Lode, and of fuchsite in one example in the Porcupine District, led Knopf and Burrows, respectively, to the inference that the chromium had its origin in these rocks, and it would obviously be difficult to prove otherwise. We may note however, that arguments by Sampson (1929) and Ross (1929) point to the fact that chromium in chromite of ultrabasic intrusives is not

always indigenous in such rocks and may have been introduced as *late* chromite by hydrothermal solutions.

Chromium derived from magmatic solutions

The great majority of occurrences of chrome-micas suggest strongly a deriviation in part from hydrothermal solutions arising from magmas. In only one case of this type cited by Hutton (1942), is fuchsite considered the result of "chromium metasomatism of quartz—feldspathic schists by emanations from deep-seated ultrabasic intrusives." One example has already been noted (Ödman) where chrome mica is closely related to a lamprophyre dyke but the mineralization at Boliden is attributed to the Revsund granite outcropping south of the mine. In all others the solutions are attributed to cooling siliceous magmas ranging from pegmatite quartz-porphyry to granite.

Two occurrences in S. E. Manitoba show fuchsite associated with pegmatite. According to Stanton[3] fuchsite occurs in pegmatite zones in the granite near the Poundmaker vein which is also reported to contain chrome mica. The Pointe du Bois fuchsite is developed in mica schist along a pegmatite dyke and has associated with it chromite, some quartz and dark red rutile.

In the Larder Lake district Cooke (1922) has noted spatial relations between the chrome-mica-carbonate alteration and pegmatitic dykes (McGarry Twp.) and quartz porphyry (McVittie Twp.), and in the latter case considers the presence of carbonates in a replaced fragment of country rock within a dyke, evidence that the solutions came from the dyke itself. After noting the absence of this alteration adjacent to red syenite porphyries, syenite and diorite of the Kirkland Lake district, he concludes that wet magmas of the type supplying pegmatite, quartz porphyry and abundant quartz veins were the source. Jenny (1941) at the Omega mine in this district, attributes the solutions which caused the carbonate alteration to the same magma that produced the intrusives other than granite, and that they were introduced soon after the pegmatites.

In the Porcupine district, while many such carbonate zones appear spatially related to intrusive quartz-porphyries, some of the porphyry bodies themselves have been extensively carbonated, as at Preston East Dome Mines, and locally chrome micas are developed in or adjacent to them. The alteration is thus clearly later than some of the porphyries of this district, but since Gustafson (1945) has indicated at least two and possibly three ages of porphyry in the district it is perhaps premature

[3] Stanton, M. S., Personal communication.

to say that the alteration is younger than all of them. As indicated in the study of the Hollinger ores, a good case may be made for a direct relation between the ore-bearing solutions and the earlier or contemporaneous deposition of ankerite and chrome-mica, whatever their source. Viewing the complex alterations and mineralization of the area as a whole, there is no reason to depart from the orthodox view that the source lay in some cooling siliceous magma at depth.

It is to Partridge (1937) that we are indebted for a method of attack on the source rocks of the chrome micas (and ores which may be associated) as well as for an excellent case of their relation to granite intrusives. In both the Mashishimala and New Consort Mine occurrences of chrome mica he notes the close relation to granite contacts. Spectroscopic examination of the various minerals in many granite occurrences throughout north and northeastern Transvaal has shown traces of Cr in all.

Accordingly it may be concluded that, while locally chromiferous ultrabasic rocks may contribute Cr to the formation of chrome micas, the great majority of cases favour its derivation, as well as that of associated ore minerals, from a siliceous magmatic source. A careful spectroscopic study of the constituents of nearby acidic intrusives may aid in relating these minerals to their actual source. Such a study should be of considerable benefit where porphyries and granites of different ages may be present.

References

Berman, H., (1937): *Am. Mineral.*, **22,** 384.
Brock, R. W., (1907): *Ann. Rept. Ont. Bur. Mines,* **16,** 207.
Burrows, A. G., (1912): *Ann. Rept. Ont. Bur. Mines,* **21,** 217.
———, (1915): *Ann. Rept. Ont. Bur. Mines,* **24** (pt. 3), 15.
———, (1924): *Ann. Rept. Ont. Dept. Mines,* **33** (pt. 2), 39.
Burwash, C. M., (1935): *Ann. Rept. Ont. Dept. Mines,* **44** (pt. 8), 17.
Buttenbach, H., (1919): *An. de la Soc. Geol. de Belg.,* **42,** 93.
Cooke, H. C., (1922): *Geol. Surv. Canada,* Mem. **131,** 48–51.
Chester, A. H., (1887): *Am. Jour. Sci.,* **33,** 284.
Damour, A., (1882): *Bull. Soc. Min.,* **5,** 97; *Zeits. Kryst.,* **7,** 17.
Dana, J. D., (1882): *System of Mineralogy,* ed. 5, New York.
Dana, E. S., (1892): *System of Mineralogy,* ed. 6, New York.
Dyer, W. S., (1935): *Ann. Rept. Ont. Dept. Mines,* **44** (pt. 2), 12, 35, 38.
Fales, H. A., (1925): *Quantitative Chemical Analysis.*
Ferguson, H. F., (1929): *Econ. Geol.,* **24,** 127.
Ferguson, R. B., (1943): *Univ. Toronto Studies, Geol. Series,* no. **48,** 31.
Gill, A. C., (1889): *Johns-Hopkins Univ. Circ.,* no. **75,** 100.
Groves, A. W., (1937): *Silicate Analysis,* London.
Gustafson, J. K., (1945): *Econ. Geol.,* **40,** 148.
Harvie, R., (1911): *Jour. Can. Min. Inst.,* **14,** 168.
Hawley, J. E., (1926): *Ann. Rept. Ont. Dept. Mines,* **35** (pt. 6), 10.
———, (1929): *Ann. Rept. Ont. Dept. Mines,* **38** (pt. 6), 36.

———, (1931): *Ann. Rept. Que. Bur. Mines* (pt. **B**), 46.
Hendricks, S. B., and Jefferson, M. E., (1939): *Am. Mineral.* **24,** 729–771.
Hillebrand, W. F., (1900) *U. S. Geol. Surv. Bull.* **167,** 74.
Hopkins, P. E., (1915): *Ann. Rept. Ont. Bur. Mines,* **27** (pt. 1), 196.
———, (1919): *Ann. Rept. Ont. Bur. Mines,* **28** (pt. 2), 73.
———, (1924): *Ann. Rept. Ont. Dept. Mines,* **33** (pt. 3), 29.
Hoffman, G. C., (1892–3): *Rept. Geol. Surv. Canada,* **6,** 27R.
Hutton, C. O., (1940): *New Zealand Jour. Sci. Techn.,* Sec. B., **21,** 330–333.
———, (1942): *Trans. Roy. Soc. New Zealand,* **72,** 53–68.
Jackson, W. W., and West, J., (1930): *Zeit. Krist.,* **76,** 221–227.
Jenny, C. P. (1941): *Econ. Geol.,* **36,** 444–445.
Knopf, A., (1929): *U. S. Geol. Surv.,* Prof. Paper, **157,** 38.
Klement, C., (1888): *Bull Mus. Belg.,* **5,** 164.
Larsen, E. S., and Berman, H., (1934): *U. S. Geol. Surv. Bull.* **848,** 165–171.
Mauguin, C., (1927): *Compt. Rend. Ac. Sci.,* Paris, **185,** 288–291.
Moore, E. S., (1936): *Ann. Rept. Ont. Dept. Mines,* **45** (pt. 6), 16.
Ödman, O. H., (1938): *Geol. Fören. Förhandl., Bd.* **60,** H. 2.
———, (1941): *Sveriges. Geol. Undersökning,* **35,** 1.
Partridge, F. C., (1937): *Trans. Geol. Soc. S. Africa,* **39,** 457–460.
Pauling, L., (1930): *Proc. Nat. Acad. Sci.,* **16,** 123.
Penfield, S. L., (1893): *Am. Jour. Sci.,* **36,** 288.
Prior, G. T., (1908): *Mineral. Mag.,* **15,** 385.
Ross, C. S., (1929): *Econ. Geol.,* **24,** 641–645.
———, (1931): *Econ. Geol.,* **26,** 540–545.
Sampson, E., (1929): *Econ. Geol.,* **24,** 632–641.
Schaller, W. T., (1916): *U. S. Geol. Surv.,* Bull. **610,** 139–140.
Simpson, E. S., (1935–36): *Jour. Roy. Soc. W. Australia,* **22.**
Silliman, B., (1868): *Cal. Acad. Sci.,* **3,** 380.
Spence, H. S., (1930): *Mica, No.* **701.** *Mines Br., Dept. Mines, Can.,* 88.
Szadeczky-Kardoss, E., (1937): *Math. Naturw. Anz. ungar Akad. Wiss.,* **56.**
———, (1937): *Mat. Term.-tub Ertesitö,* **56,** 346–351.
———, (1937): *Publ. Dep. Min. Met. Roy. Hung. Palatine—Joseph Univ.,* **9,** 186–191.
Thomson, J. E., (1935): *Ann. Rept. Ont. Dept. Mines,* **44** (pt. 4), 47–80.
———, (1936): *Ann. Rept. Ont. Dept. Mines,* **45** (pt. 3), 28, 50.
Turner, H. W., (1895): *Am. Jour. Sci.,* **49,** 374–380.
Washington, H. S., (1930): *The Chemical Analysis of Rocks,* 4th Ed., New York.
Wherry, E. T., (1916): *Proc. U. S. Nat. Mus.,* **49,** 465.
Whitmore, D. R. E. (1940): Unpublished report to Nat. Res. Council, Ottawa.
Wilson, M. E., (1909): *Geol. Surv. Canada, Sum. Rept.,* 175.
———, (1912): *Geol. Surv. Canada,* Mem. **17 E,** 22.
Winchell, A. N., (1925): *Am. Jour. Sci.,* **9,** 415–430.
———, (1927): *Am. Mineral.* **12,** 267.
Volk, G. W. (1939): *Am. Mineral.,* **24,** 255.

MICROSCOPIC QUARTZ CRYSTALS IN BROWN COAL, VICTORIA

George Baker,
University of Melbourne, Victoria, Australia.

Abstract

Minute, doubly-terminated crystals of quartz showing simple crystallographic forms occur in patches in the Tertiary Brown Coal at two localities in Victoria. They have crystallised from solutions derived either from the magma of the overlying basalt flows, or from vadose waters.

Occurrence

Underground mining operations at the Parwan Colliery, 27 miles W. N.W. of Melbourne, have revealed that the upper 12 feet of the hard, earthy Parwan brown coal seam is impregnated with minute, doubly-terminated quartz crystals. The top of the seam is exposed in the inclined main heading leading northwards from the shaft.

The coal seam, which is Miocene in age (Parr, 1942), is about 100 feet thick, and lies at a depth of 405 feet below the surface. Immediately above the seam is a 9 foot thick bed of pyritic sands, partly cemented, but largely so unconsolidated that it rills down into the workings if the top of the seam is broken through. Above the sands are fossiliferous marine clays, which are capped by two thick flows of Newer Volcanic basalt, of a total thickness amounting to approximately 250 feet. A basaltic dyke, about 3 feet wide, has intruded the coal seam in the area impregnated with quartz crystals. The coal adjacent to the dyke developed minute shrinkage cracks which were filled with threads of basalt.

The quartz crystals are most abundantly developed at the roof of the seam, and diminish in both quantity and size with increase in depth below it, being practically absent at 12 feet below the roof. Ash determinations made at the Victorian Mines Department Laboratory show that in the top six feet of coal the ash, which consists chiefly of quartz crystals varies from 14.25% to 26.95%, while in coal from 6 to 12 feet below the top of the seam, the ash content is only 7%. The average ash content of the coal as mined (at 30 feet below the top of the seam) is 5%.

The decrease in the size of the crystals with increasing depth below the top of the seam, is shown by the following measurements:

Depth Below Top of Seam	Size Range in Mm.	Average Size in Mm.
0 feet	0.10×0.05–2.0 ×0.75	0.50×0.20
3 feet	0.08×0.05–0.54×0.32	0.32×0.13
5 feet	0.05×0.025–0.29×0.13	0.11×0.05
7 feet	0.03×0.015–0.16×0.08	0.08×0.03
9 feet	0.03×0.015–0.11×0.05	0.06×0.02

In like manner, the decrease in quantity of quartz crystals with increase in depth, is indicated by the fact that three times as much quartz, by weight, occurred 3 feet below the top of the seam than at two feet lower.

At the top of the seam there are some patches in which the crystals are so crowded that the growing crystals obstructed one another, forming masses of interlocking quartz crystals, and giving rise locally to "quartzite" and to small veinlets. Some of the "quartzite" patches had associated rosettes of aragonite needles on their surfaces.

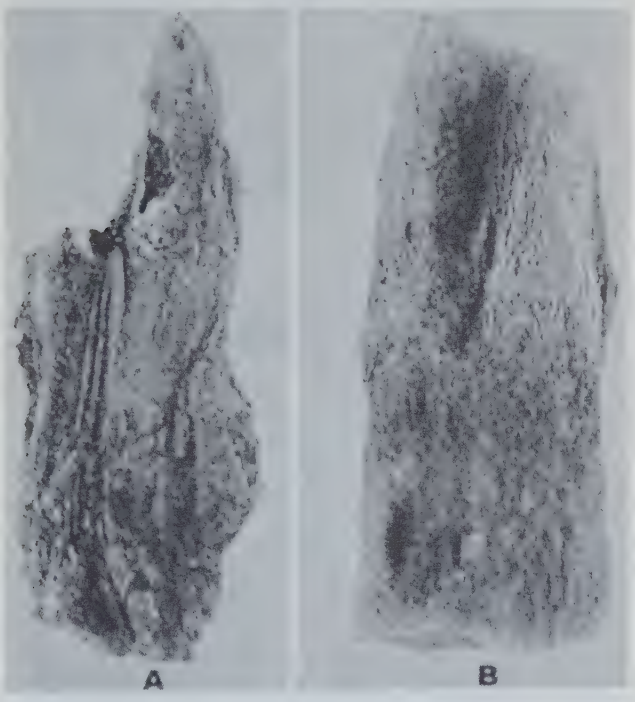

FIG. 1. Wood replaced by double-ended quartz crystals. The woody structure is still evident. Part of a log originally 12 inches long and 8 inches in diameter, from the Old Shaft mine dump, Altona. A—×0.45; B—×0.48. (A. A. Baker collection. Photo by Miss M. L. Johnston.)

A similar development of quartz crystals in Tertiary (Miocene) brown coal is known to occur at Altona, approximately 9 miles W.S.W. of Melbourne. This occurrence could not be observed underground, since the Altona brown coal mine is now closed, but specimens from the dump at the Old Shaft, differ from the Parwan specimens only in that the quartz crystals are generally somewhat larger, and have only been ob-

served so far replacing logs of fossil wood (Figs. 1 and 2). Similar, minute quartz crystals occur on the surface of a white coloured, completely silicified fragment of a tree trunk collected on the same mine dump, but which most probably came from siliceous deposits above the coal.

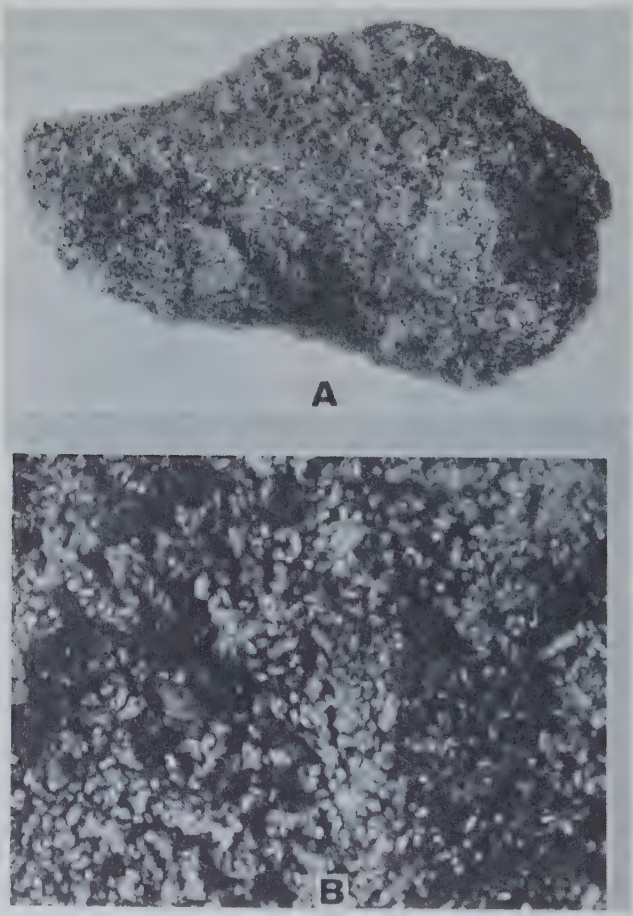

FIG. 2. A—portion broken from the interior of one of the samples depicted in Fig. 1. Woody structure not evident. ×0.49. B—enlarged portion of A, above, showing mass of minute quartz crystals. ×3. (F. S. Colliver collection. Photographs by Miss M. L. Johnston.)

These occurrences are of especial interest, not only because of the infrequent formation of quartz crystals in brown coal, but also because of the great multitude of freely-occurring, doubly-terminated quartz crys-

tals present. Doubly-terminated quartz crystals are usually of some rarity under any conditions.

Form of Crystals

The quartz crystals in the Victorian Tertiary brown coal from Parwan and Altona are low temperature forms which crystallised below 575° C. in the hexagonal trapezohedral hemihedral symmetry group (i.e., the Trapezohedral Class, Quartz Type).

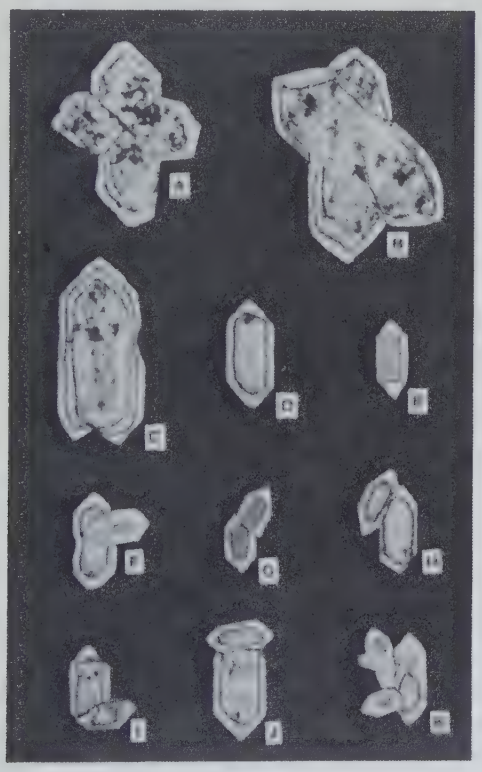

Fig. 3. Quartz crystals from brown coal, Parwan Colliery.
Photographed under crossed nicols. ×55.
A and B—interpenetration (cruciform) twins.
C, D and E—single double-ended crystals.
F, G, H and J—double-ended crystals with outgrowths.
I—contact twin.
K—irregular aggregate built up from several outgrowths. (Photographs by Miss M. L. Johnston.)

The crystals are coated to some extent with carbonaceous material, but on burning and separating the resultant greyish-white ash, the quartz crystals are seen to be principally clear and colourless, i.e., they are microscopic crystals of *rock crystal*. Of the many thousands of these quartz crystals examined under the microscope, the majority are doubly-terminated (Fig. 3; C, D and E), and many of them are almost geometrically perfect in shape (Fig. 4 No. 1).

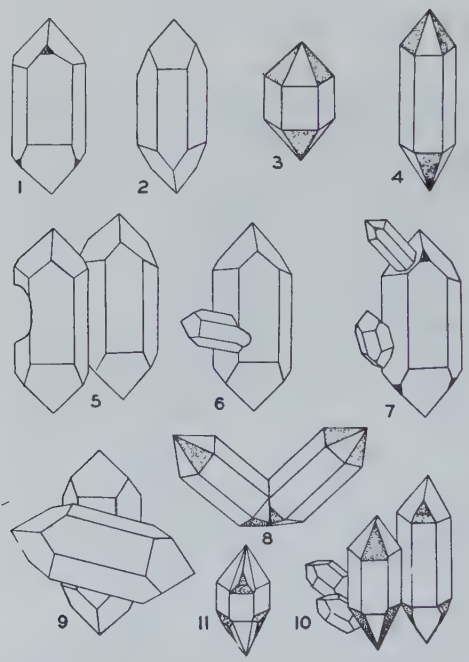

FIG. 4. Sketch diagrams of doubly-terminated, twinned and aggregated quartz crystals from the top of the Parwan Colliery brown coal.

The crystallographic faces and pecularities of habit of the quartz crystals are generally similar at both localities. Because of greater ease of separation of the quartz crystals from brown coal than from replaced wood, most of the sketches depicted in Fig. 4 represent examples from the Parwan Colliery.

The crystallographic forms are typically those of the rhombohedral-trapezohedral class. The most common form is that of the unit prism, terminated at both ends, often with equally developed faces of the positive first order rhombohedron ($h0\bar{h}1$), as shown in Fig. 4, no. 2, but occasionally with unequally developed faces of the same form. Where not doubly-terminated, the quartz crystals have broken away from clusters

during preparation of the sample.

In some instances, the negative rhombohedron ($0h\bar{h}1$) is the dominant of the rhombohedron faces possible in the quartz symmetry group, but is modified by small faces of the positive rhombohedron (Fig. 4, no. 1). In few crystals are the positive and negative rhombohedra equally developed, and in them, the long axis of the combined forms may be short compared to the length of the lateral axes (Fig. 4, no. 3), or considerably longer than the lateral axes (Fig. 4, no. 4). Seldom do crystals possess two forms of the positive rhombohedron, as in the right-hand crystal sketched in Fig. 4, no. 10.

Whereas the greater number of the quartz crystals in the brown coal are free, doubly-terminated crystals, clusters are occasionally developed, more particularly in the replaced wood from Altona and in the occasional "quartzite-like" patches at the top of the seam in the Parwan brown coal. Among the clusters are irregular aggregates of up to four and five quartz crystals (Fig. 3 (K)).

Parallel growths are occasionally present; in them, two or more doubly-terminated quartz crystals are usually attached by means of the prism faces (Fig. 4, no. 5). In some instances, smaller parallel growths are attached to larger parallel growths, but they usually grow out from the larger growths at an acute angle (Fig. 4, no. 10). Where doubly-terminated crystals occur as attached pairs, the axis of each individual crystal may vary from being parallel to that of the other, as in parallel growths, to positions where they are almost at right angles (Fig. 4, no. 9; and Fig. 3 (J)). Examples such as these have one perfect crystal embedded in the other, and when broken away, concavities are invariably left in one crystal, as indicated in the left-hand crystal of Fig. 4, no. 5. Crystals showing two, rarely three such concavities, obviously possessed two and three embedded quartz crystals.

Sometimes smaller crystals grow out from various positions on larger crystals, principally from one of the prism faces of larger, doubly-terminated crystals, as in Fig. 4, no. 6; and in Fig. 3(F). They seldom grow out from a rhombohedral face of a larger crystal, as in Fig. 4, no. 7; and in Fig. 3(G). These smaller outgrowths, which sometimes appear "chimney-like," are not doubly-terminated crystals. A few outgrowths from the larger doubly-terminated crystals, themselves occasionally possess still smaller outgrowths. The outgrowths characteristically display similar types and similar numbers of crystal faces as the host crystal.

Occasional interpretation twins of the type shown in Fig. 3 (A and B), and contact twins of the type depicted in Fig. 4, no. 8, and in Fig. 3(I) are present. In the contact twins, the vertical axes of each twin half intersect at approximately 85°.

None of the crystals showed the pyramidal habit of large doubly-terminated quartz crystals. Crystallographic faces unrepresented in these minute crystals from brown coal are those of the basal pinacoid, trapezohedra and trigonal pyramids, consequently enantiomorphous forms could not be detected.

Where siliceous solutions became concentrated in occasional patches at the top of the 100 feet thick brown coal seam at Parwan, crystallisation caused considerable crowding together, so that interference of the

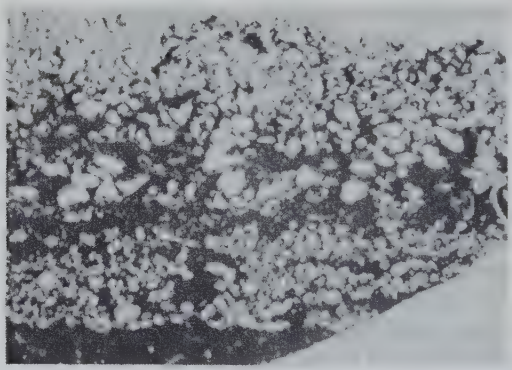

FIG. 5. Microsection of top of brown coal seam, Parwan Colliery. Ordinary light. ×3.5. Showing gradation in size of quartz crystals from above downwards. A small veinlet of silica appears in the bottom right-hand portion of the photograph. (Photo by Miss M. L. Johnston.)

growing crystals with one another prevented the growth of well-developed double-ended crystals. As a result, such patches consist mainly of masses of interlocking quartz crystals, and these are coarser in size at the top, and much smaller an inch or two lower (Fig. 5). Two small veinlets of quartz were observed in a thin section of this material; they extended to the larger crystals situated at the top of the coal seam. Carbonaceous inclusions occurred along cracks in some of the quartz crystals. In areas of somewhat lesser concentration of independent quartz crystals, small splinters of woody tissue adjacent to growing quartz crystals were bent outwards into the less resistant brown coal by the forces of crystallisation. Several fragments of wood occur where the cells have been infilled with silica, resulting in pseudomorphs by infiltration, but the cell wall tissue has not been molecularly replaced, remaining as partially coalified wood.

At the junction of the upper limit of the coal seam and the sands which form the roof of the seam, some of the quartz crystals are rounded: these

examples are apparently waterworn grains which have become embedded in the topmost layer of coal. A short distance below, the quartz grains embedded in the coal are surrounded by a narrow zone of carbonaceous material, and this in turn is surrounded by a further layer of quartz forming crystal outlines, as seen in Fig. 5. Such occurrences provide examples of authigenic quartz growing in optical continuity with allothigenic quartz. They are confined to the top inch or so of the coal. All other quartz crystals in the coal below this level, are entirely authigenic in character, and they form the well-developed, doubly-terminated, clear, colourless quartz crystals which have grown in place.

Origin

The growth of introduced quartz crystals in brown coal seams is of interest in providing small scale examples of the growth of quartz veins by force of crystallisation in the manner suggested by Taber (1919), as a result of his laboratory experiments on vein formation, and advocated by Stillwell (1918, p. 27) for the development and growth of spur veins in the Bendigo goldfield, Victoria.

The distribution of the quartz crystals in the Parwan brown coal leaves little doubt that the siliceous solutions from which they crystallised migrated along the top of the coal seam, through the sand bed above the coal, cementing the sands in parts immediately above the seam, and soaking downwards into the coal. The brown coal, being relatively porous, and containing a high proportion (50% at each locality) of readily displaceable water, provided an ideal situation for the growth of perfect minute quartz crystals.

Crystallisation developed at innumerable points, the size of the resultant crystals being governed by the available supply of silica in solution. As the crystals grew, they thrust aside the relatively plastic coal, and where the supply of silica was adequate, such as along parts of the top of the seam, the crystals grew until they mutually obstructed one another and practically all the coal originally present was pushed aside. Where more porous areas, such as fragments of logs of wood, were reached by the siliceous solutions, greater amounts of infiltration and replacement took place, and the wood ultimately became transformed into a mass of quartz crystals with small amounts of entrapped carbonaceous material. Still further replacement of such areas, ultimately led to the complete expulsion of carbonaceous matter, and the wood fragments became transformed into pseudomorphs consisting entirely of silica crystals, with occasional, small, doubly-terminated quartz crystals attached to the exterior surfaces.

The source of the siliceous solutions can only be surmised. The fact

that gravels and sands underlying basalt flows in Victoria and New South Wales are commonly silicified and converted to quartzites (sometimes known as "Grey Billy"), suggests that the basaltic lavas may have been the source of the solutions. The possibility cannot be dismissed, however, that the solutions may be ordinary circulating subterranean solutions saturated in silica.

Acknowledgments

The author is indebted to the Director of the Victorian Geological Survey, Mr. W. Baragwanath, for the samples of quartz-bearing brown coal from the Parwan Colliery, to Mr. F. S. Colliver and Mr. A. A. Baker for the loan of quartz-replaced fossil wood collected in 1937 from the old Altona Mine, and to Dr. A. B. Edwards for assistance with the manuscript and discussions on the problem.

References

Parr, W. J. (1942), The age of the lignite deposits at Parwan: *Mining and Geol. Journ.*, **2**, *no.* 6, 363–364.

Stillwell, F. L. (1918), The factors influencing gold deposition in the Bendigo Goldfield: Part II. *Austr. Comm. Advisory Council Sci. and Industry. Bull.*, **8**, 7–47.

Taber, S. (1919), Mechanics of vein formation: *Trans. Am. Inst. Min. and Met.*, **61**, 3–41.

COMPUTATION OF INTERFACIAL ANGLES, INTERZONAL ANGLES, AND CLINOGRAPHIC PROJECTION BY MATRIX METHODS

W. L. Bond,

Bell Telephone Laboratories, Murray Hill, New Jersey.

Abstract

A way of setting up the general crystallographic axes a, b, c on unit orthogonal axes x, y, z is used to afford a matrix method of computing interfacial angles and zonal angles. It also affords a method of making clinographic projections.

Introduction

The problems of crystal geometry are mainly problems of relations between directions in space. The "direction" of a crystal face is most conveniently characterized by the direction of a line perpendicular to the face, this line being called the normal of the face. It is often very helpful to restrict this normal to unit length, in which case it is called a unit normal. A unit normal, then, is a line having both length and direction and hence fits the definition of a vector. In specifying a group of vectors we may state their lengths and directions very conveniently in terms of a set of three non-coplanar vectors which intersect at a point called the origin. We shall always call these three vectors the base vectors to avoid confusing them with the other vectors. Let us assume that we have base vectors $\boldsymbol{a}$, $\boldsymbol{b}$, and $\boldsymbol{c}$ of length a, b, and c units, respectively, and wish to specify a vector $\boldsymbol{V}$ in terms of $\boldsymbol{a}$, $\boldsymbol{b}$, and $\boldsymbol{c}$. We imagine moving $\boldsymbol{V}$ about in space, without changing its direction, until the tail end of $\boldsymbol{V}$ is at the origin. We now find that we can reach the head end of $\boldsymbol{V}$ by taking V_1 steps of length a along $\boldsymbol{a}$, then taking V_2 steps of length b parallel to $\boldsymbol{b}$ and finally V_3 steps of length c parallel to $\boldsymbol{c}$, see Fig. 1. These three numbers V_1, V_2, and V_3 are the components of the vectors $\boldsymbol{V}$ on the $\boldsymbol{a}\,\boldsymbol{b}\,\boldsymbol{c}$ basis. We shall denote this fact by means of the equation:

$$(\boldsymbol{V})_a = \begin{pmatrix} V_1 \\ V_2 \\ V_3 \end{pmatrix}_a$$

where the subscripts a remind us that these components are stated on the $\boldsymbol{a}\,\boldsymbol{b}\,\boldsymbol{c}$ basis which we shall henceforth call the a basis.

On another system with base vectors $\boldsymbol{d}\,\boldsymbol{e}\,\boldsymbol{f}$ the components of $\boldsymbol{V}$ will be quite different. Let us say that on this system, which we shall call the d basis, the components are V_1', V_2', and V_3'; that is:

$$(\boldsymbol{V})_d = \begin{pmatrix} V_1' \\ V_2' \\ V_3' \end{pmatrix}_d .$$

If we know the relationship between the a and d bases, we can compute the components of any vector $\boldsymbol{V}$ on one basis given its components on the other. This relationship between bases is most conveniently given in

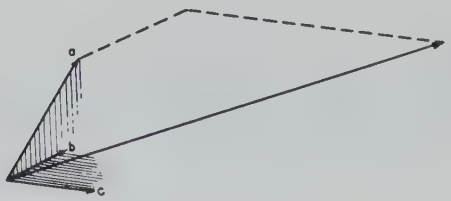

FIG. 1. Illustration of the vector $\begin{pmatrix} 1 \\ 2 \\ 3 \end{pmatrix}_a$.

terms of a matrix, i.e., a rectangular array of numbers (the numbers being the components of one basis on the other). As an illustration of a matrix, and also of a special kind of "multiplication" known as matrix multiplication, we multiply the vector

$$(\boldsymbol{V})_a = \begin{pmatrix} 1 \\ 2 \\ 3 \end{pmatrix} \text{ by the matrix } m = \begin{pmatrix} 4 & 5 & 6 \\ 7 & 8 & 9 \\ 10 & 11 & 12 \end{pmatrix}$$

$$m(\boldsymbol{V})_a = \begin{pmatrix} 4 & 5 & 6 \\ 7 & 8 & 9 \\ 10 & 11 & 12 \end{pmatrix}\begin{pmatrix} 1 \\ 2 \\ 3 \end{pmatrix} = \begin{pmatrix} 4\times 1 + & 5\times 2 + & 6\times 3 \\ 7\times 1 + & 8\times 2 + & 9\times 3 \\ 10\times 1 + 11\times 2 + & & 12\times 3 \end{pmatrix} = \begin{pmatrix} 32 \\ 50 \\ 68 \end{pmatrix}$$

which is a new vector. It is seen that the resultant components are found by summing products in a systematic way, namely, the first resulting component is the sum of the terms of the first row of the matrix multiplied in turn by the components of the vector, the second is the sum of the terms of the second row of the matrix multiplied in turn by the components of the vector, and similarly for the last component. After a little practice this kind of "multiplication" becomes purely mechanical. In terms of this kind of multiplication we now give the equation that allows us to compute the components on one basis given the components on the other basis and given the matrix connecting the bases:

$$(\boldsymbol{V})_d = M(\boldsymbol{V})_a. \tag{1}$$

As an example, we write the matrix that gives the relationship between a simple set of vectors $\mathbf{x}, \mathbf{y}, \mathbf{z}$ (all of unit length and mutually perpendicular) and the set of vectors $\boldsymbol{a}\ \boldsymbol{b}\ \mathbf{c}$ taken as the axes of a triclinic crystal,

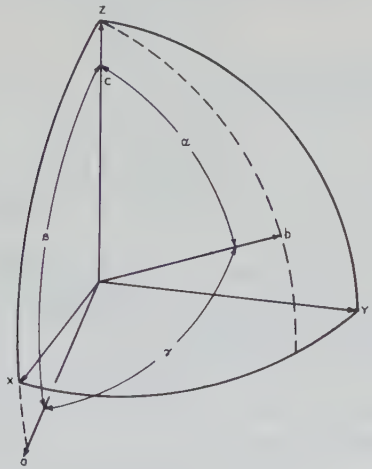

FIG. 2. Triclinic system as related to x system.

b being equal to unity. If we take $\mathbf{c}$ as lying along $\boldsymbol{z}$ and let $\boldsymbol{a}$ lie in the plane of $\mathbf{x}$ and $\boldsymbol{z}$ (see Fig. 2)* we get the matrix:

$$M = \begin{pmatrix} a \sin\beta & v_1 & 0 \\ 0 & v_2 & 0 \\ a\cos\beta & \cos\alpha & c \end{pmatrix} \tag{2}$$

where α, β and γ are the triclinic angles of the crystal and where

$$v_1 = \frac{\cos\gamma - \cos\alpha\cos\beta}{\sin\beta}$$

and

$$v_2 = \frac{\sqrt{1 + 2\cos\alpha\cos\beta\cos\gamma - (\cos^2\alpha + \cos^2\beta + \cos^2\gamma)}}{\sin\beta}.$$

Here β is taken as the obtuse angle of the regular triclinic axes. In this matrix, M, the columns are the components of the vectors $\boldsymbol{a}$, $\boldsymbol{b}$ and $\mathbf{c}$ on the x basis, that is:

$$(\boldsymbol{a})_x = \begin{pmatrix} a\sin\beta \\ 0 \\ a\cos\beta \end{pmatrix}_x, \quad (\boldsymbol{b})_x = \begin{pmatrix} v_1 \\ v_2 \\ \cos\alpha \end{pmatrix}_x \text{ and } (\mathbf{c})_x = \begin{pmatrix} 0 \\ 0 \\ c \end{pmatrix}_x.$$

* The x basis is convenient not only in performing certain crystallographic computations, as will be shown below, but also as a basis to which to refer the vectors and tensors involved in the expression of elastic and electric properties of crystals.

As an illustration of the use of equation (1) we will compute the components on the x basis of a vector

$$(\boldsymbol{V})_a = \begin{pmatrix} 1 \\ 0 \\ 1 \end{pmatrix}_a .$$

By matrix multiplication we see that:

$$(\boldsymbol{V})_x = \begin{pmatrix} a\sin\beta & v_1 & 0 \\ 0 & v_2 & 0 \\ a\cos\beta & \cos\alpha & c \end{pmatrix} \begin{pmatrix} 1 \\ 0 \\ 1 \end{pmatrix} = \begin{pmatrix} a\sin\beta \\ 0 \\ a\cos\beta + c \end{pmatrix}_x$$

To solve the inverse problem, namely, given $(\boldsymbol{V})_x$ to find $(\boldsymbol{V})_a$ we use the reciprocal matrix M^{-1}, the columns of which are the components of $\boldsymbol{x}\,\boldsymbol{y}$ and $\boldsymbol{z}$ on $\boldsymbol{a}$ $\boldsymbol{b}$ and $\mathbf{c}$, respectively.

$$M^{-1} = \begin{pmatrix} \dfrac{1}{a\sin\beta} & \dfrac{-v_1}{av_2\sin\beta} & 0 \\ 0 & 1/v_2 & 0 \\ \dfrac{-\cot\beta}{c} & \dfrac{v_1\cot\beta - \cos\alpha}{v_2 c} & 1/c \end{pmatrix} \tag{3}$$

we may easily verify that $M^{-1}\begin{pmatrix} a\sin\beta \\ 0 \\ a\cos\beta + c \end{pmatrix}_x = \begin{pmatrix} 1 \\ 0 \\ 1 \end{pmatrix}_a .$

We need one more variant of these matrices, namely the transposed matrix $\overline{M}$. It is merely the matrix re-written so that the columns appear as rows and the rows as columns. For example, the transposed M^{-1} matrix is:

$$\overline{M}^{-1} = \begin{pmatrix} \dfrac{1}{a\sin\beta} & 0 & \dfrac{-\cot\beta}{c} \\ \dfrac{-v_1}{av_2\sin\beta} & 1/v_2 & \dfrac{v_1\cot\beta - \cos\alpha}{v_2 c} \\ 0 & 0 & 1/c \end{pmatrix} \tag{4}$$

This can be read "M bar reciprocal."

Vectors themselves can be regarded as one-column three-row, or one-row three column, matrices. Indeed they have implicitly been so regarded while we subjected them to matrix multiplication. Thus as a special case of the transposed matrix we have the transposed vector, for instance $(\overline{V})_x = (V_1,\ V_2,\ V_3)_x$.

On the x basis some equations become quite simple. For example, the cosine of the angle between two unit vectors $(\boldsymbol{V})_x$ and $(\boldsymbol{W})_x$ is given by matrix multiplication as:

$$\cos \epsilon_w{}^v = (\bar{V})_x(W)_x \tag{5}$$

which is the matrix notation for the familiar vector definition of scalar product. To illustrate we take the two unit vectors

$$(V)_x = \begin{pmatrix} 1/2 \\ \sqrt{3}/2 \\ 0 \end{pmatrix} \quad \text{and} \quad (W)_x = \begin{pmatrix} 0 \\ -1/2 \\ \sqrt{3}/2 \end{pmatrix}.$$

$$\text{Cos } \epsilon_w{}^v = \left(\frac{1}{2},\ \frac{\sqrt{3}}{2},\ 0\right)_x \begin{pmatrix} 0 \\ -1/2 \\ \sqrt{3}/2 \end{pmatrix}_x = \frac{1}{2} \times 0 - \frac{1}{2} \times \frac{\sqrt{3}}{2} + 0 \times \frac{\sqrt{3}}{2},$$

or $$\cos \epsilon_w{}^v = \frac{-\sqrt{3}}{4}, \quad \text{whence} \quad \epsilon_w{}^v = 115°40'.$$

In the order to utilize equation (5), if the vectors on the x basis are not of unit length, we must make them so. We can do this by dividing each vector by its length. The length of a vector is the square root of the sum of the squares of its components on the x basis. This process we shall call "normalizing."* It will be symbolized by the superscript n after a vector. For example, the vector

$$V = \begin{pmatrix} 1 \\ 2 \\ 3 \end{pmatrix}_x$$

normalizes to

$$(V)_x{}^n = \begin{pmatrix} 1 \\ 2 \\ 3 \end{pmatrix}_x \frac{1}{\sqrt{1 + 2^2 + 3^2}} = \begin{pmatrix} 1/\sqrt{14} \\ 2/\sqrt{14} \\ 3/\sqrt{14} \end{pmatrix}_x.$$

The case of triclinic crystals being the most complicated case in crystallography, we should expect the matrices for simpler crystal systems to be simpler than the matrix M, as indeed they are. If we put $\alpha = \gamma = 90°$ we meet the conditions of the monoclinic system. Equations (2) and (3) give the respective forms for the monoclinic system:

$$M_m = \begin{pmatrix} a \sin \beta & 0 & 0 \\ 0 & 1 & 0 \\ a \cos \beta & 0 & c \end{pmatrix}. \tag{6}$$

$$M_m{}^{-1} = \begin{pmatrix} \dfrac{1}{a \sin \beta} & 0 & 0 \\ 0 & 1 & 0 \\ \dfrac{-\cot \beta}{c} & 0 & 1/c \end{pmatrix}. \tag{7}$$

* Normal is used in two senses. As first used, a line normal to a plane is perpendicular to it. When we normalize it we reduce it to a "Norm," namely unit length.

If we put $\beta = 90°$ we find the forms for the orthorhombic system:

$$M_0 = \begin{pmatrix} a & 0 & 0 \\ 0 & 1 & 0 \\ 0 & 0 & c \end{pmatrix}. \tag{8}$$

$$M_0^{-1} = \begin{pmatrix} 1/a & 0 & 0 \\ 0 & 1 & 0 \\ 0 & 0 & 1/c \end{pmatrix}. \tag{9}$$

If, in equations (2) and (3) we put $a = b = 1$, $\alpha = \beta = 90°$ and $\gamma = 120°$, we find the form for the hexagonal system:

$$M_h = \begin{pmatrix} 1 & -1/2 & 0 \\ 0 & \sqrt{3}/2 & 0 \\ 0 & 0 & c \end{pmatrix}. \tag{10}$$

$$M_h^{-1} = \begin{pmatrix} 1 & 1/\sqrt{3} & 0 \\ 0 & 2/\sqrt{3} & 0 \\ 0 & 0 & 1/c \end{pmatrix}. \tag{11}$$

For completeness we give the matrices for the little used rhombohedral or trigonal system:

$$M_r = \begin{pmatrix} 3/2 & -3/2 & 0 \\ \sqrt{3}/2 & \sqrt{3}/2 & -\sqrt{3} \\ c & c & c \end{pmatrix}. \tag{12}$$

$$M_r^{-1} = \tfrac{1}{3}\begin{pmatrix} 1 & 1/\sqrt{3} & 1/c \\ -1 & 1/\sqrt{3} & 1/c \\ 0 & -2/\sqrt{3} & 1/c \end{pmatrix} \tag{13}$$

where c (the same c as that in the hexagonal system) is given in terms of the rhombohedral angle α by

$$c = \frac{\sqrt{1 \cdot 5 + 3\cos\alpha}}{1 - \cos\alpha}. \tag{14}$$

In equations (8) and (9) we put $a = 1$ to obtain the forms for the tetragonal system:

$$M_t = \begin{pmatrix} 1 & 0 & 0 \\ 0 & 1 & 0 \\ 0 & 0 & c \end{pmatrix}. \tag{15}$$

$$M_t^{-1} = \begin{pmatrix} 1 & 0 & 0 \\ 0 & 1 & 0 \\ 0 & 0 & 1/c \end{pmatrix}. \tag{16}$$

Finally, we put $c=1$ to obtain the matrix for the isometric system:

$$M_i = \begin{pmatrix} 1 & 0 & 0 \\ 0 & 1 & 0 \\ 0 & 0 & 1 \end{pmatrix} = M_i^{-1}. \tag{17}$$

In the following, general rules will be stated in terms of the matrix M, it being understood that the appropriate subscript will be supplied according to the system of the crystal being studied.

A great aid to understanding crystal problems is the concept of a vector basis reciprocal to the a basis. We shall call this the A basis. Its base vectors are $\boldsymbol{A}$, $\boldsymbol{B}$ and $\boldsymbol{C}$. On the x basis the components of $\boldsymbol{A}$ are the three terms of the first column of $\overline{M}^{-1}$, of $\boldsymbol{B}$ are the terms of the second column, and of $\boldsymbol{C}$ are those of the last column. $\boldsymbol{A}$ is perpendicular to $\boldsymbol{b}$ and $\boldsymbol{c}$, $\boldsymbol{B}$ to $\boldsymbol{c}$ and $\boldsymbol{a}$, $\boldsymbol{C}$ to $\boldsymbol{a}$ and $\boldsymbol{b}$. Conversely, $\boldsymbol{a}$ is perpendicular to $\boldsymbol{B}$ and $\boldsymbol{C}$, $\boldsymbol{b}$ to $\boldsymbol{C}$ and $\boldsymbol{A}$, $\boldsymbol{c}$ to $\boldsymbol{A}$ and $\boldsymbol{B}$. Given a vector $(\boldsymbol{V})_A$ on the A basis we can find its component on the x basis by means of the equation

$$(\boldsymbol{V})_x = \overline{M}^{-1}(\boldsymbol{V})_A. \tag{18}$$

The Direction of Face Normals and Interfacial Angles

A crystal face with Miller indices $(h\ k\ l)_a$ on the a basis has a normal with components on the A basis of:

$$\begin{pmatrix} h \\ k \\ l \end{pmatrix}_A$$

If we wish to convert this to the x basis we apply equation (18). This shows us how to compute the angle between any two faces, say $(h\ k\ l)$ and $(h'\ k'\ l')$ for we may write them as vectors

$$\begin{pmatrix} h \\ k \\ l \end{pmatrix}_A \quad \text{and} \quad \begin{pmatrix} h' \\ k' \\ l' \end{pmatrix}_A$$

on the A basis, then convert these normals to components on the x basis, normalize them, and multiply them together as in equation (5) to give the cosine of the angle between the plane normals, this being the angle crystallographers call the angle between planes. As an example we take rhodonite, and compute the angle between two faces. Here $a=1.0728$ $b=1$, and $c=0.6213$, $\alpha=103^\circ\ 18'$, $\beta=108^\circ\ 44'$, and $\gamma=81^\circ\ 39'$. Whence $v_1=0.07533$ and $v_2=0.97026$ so that

$$\overline{M}^{-1} = \begin{pmatrix} .98428 & 0 & .54585 \\ -.07642 & 1.0306 & .32915 \\ 0 & 0 & 1.6095 \end{pmatrix}.$$

The angle between the planes $(\bar{2}21)$ and $(\bar{2}\bar{2}1)$ is the angle between their normals $N_{\bar{2}21}$ and $N_{\bar{2}\bar{2}1}$.

$$N_{\bar{2}21} = \overline{M}^{-1}\begin{pmatrix} -2 \\ 2 \\ 1 \end{pmatrix} = \begin{pmatrix} -1.4227 \\ 2.5432 \\ 1.6095 \end{pmatrix}_x, \quad N^n_{\bar{2}21} = \begin{pmatrix} -.42737 \\ .76396 \\ .48349 \end{pmatrix}_x$$

$$N_{\bar{2}\bar{2}1} = \overline{M}^{-1}\begin{pmatrix} -2 \\ -2 \\ 1 \end{pmatrix} = \begin{pmatrix} -1.4227 \\ -1.5792 \\ 1.6095 \end{pmatrix}_x, \quad N_{\bar{2}\bar{2}1} = \begin{pmatrix} -.55360 \\ -.59231 \\ +.60637 \end{pmatrix}_x$$

$$\cos(\bar{2}21)\wedge(\bar{2}\bar{2}1) = (-.42737, .76396, .48349)\begin{pmatrix} -.53360 \\ -.59231 \\ +.60367 \end{pmatrix}$$

$$= .22804 - .45250 + .29188 = .06742$$

whence $(\bar{2}21)\wedge(\bar{2}\bar{2}1) = 86°8'$.

Direction of Edges

The zone symbol* derived from the indices of a pair of planes can be interpreted as the components, on the a basis, of a vector parallel to both planes. (It can also be interpreted as the indices, on the reciprocal basis, of a plane perpendicular to both of the original planes.) To find the components on the x basis we have only to multiply the zone symbol by the appropriate M matrix.

Angles Between Edges

To find the cosine of the angle between two edges we first "cross multiply" to obtain the two zone symbols of the edges. These are considered as vectors on the a basis and their components on the x basis are computed. These vectors are converted into unit vectors and their scalar product found. Rhodonite will again be used as an example: find the angle between the edge formed by (100) and $(\bar{2}\bar{2}1)$ and the edge formed by (100) and (110). The zone symbol of (100) and $(\bar{2}\bar{2}1)$ is:

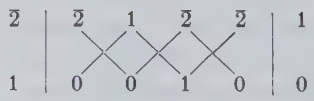

[012].

* It will be recalled that the zone symbol $[uvw]$ for the planes $(h\ k\ l)$ and $(h_1\ k_1\ l_1)$ is given by cross-multiplication according to the scheme $u = kl_1 - lk_1$, $v = lh_1 - hl_1$, $w = hk_1 - hk_1$.

Hence the edge between (100) and $(\bar{2}\bar{2}1)$ is parallel to the vector

$$\begin{pmatrix} 0 \\ 1 \\ 2 \end{pmatrix}_a .$$

The zone symbol of (100) and (110) is

[001].

Since the edge between $(\bar{2}\bar{2}1)$ and (100) is:

$$(E_{100}^{\bar{2}\bar{2}1})_a = \begin{pmatrix} 0 \\ 1 \\ 2 \end{pmatrix}, \text{ we have } (E_{100}^{\bar{2}\bar{2}1})_x = M(E_{100}^{\bar{2}\bar{2}1})_a$$

$$= \begin{pmatrix} 1.0161 & .07533 & 0 \\ 0 & .97026 & 0 \\ -.34460 & -.23005 & .6213 \end{pmatrix} \begin{pmatrix} 0 \\ 1 \\ 2 \end{pmatrix}_a = \begin{pmatrix} .07533 \\ .97026 \\ 1.0125 \end{pmatrix}_x$$

which gives the unit vector:

$$E' = \begin{pmatrix} .05364 \\ .69087 \\ .72095 \end{pmatrix}_x .$$

Similarly

$$E_{110}^{100} = \begin{pmatrix} 0 \\ 0 \\ 1 \end{pmatrix}_a = \begin{pmatrix} 0 \\ 0 \\ .6213 \end{pmatrix}_x$$

which becomes the unit vector

$$E'' = \begin{pmatrix} 0 \\ 0 \\ 1 \end{pmatrix}.$$

Finally

$$\cos E_{100}^{\bar{2}\bar{2}1} \wedge E_{110}^{100} = (001) \begin{pmatrix} .05364 \\ .69087 \\ .72095 \end{pmatrix} = .72095,$$

or the angle is 43°52′.

Clinographic Projection by Matrix Computation

An edge direction $(E)_x$ can be projected onto the plane of the clinographic projection by multiplying by the matrix:

$$K = \begin{pmatrix} \frac{-1}{\sqrt{10}} & \frac{3}{\sqrt{10}} & 0 \\ \frac{-3}{\sqrt{370}} & \frac{-1}{\sqrt{370}} & \frac{6}{\sqrt{37}} \end{pmatrix}. \tag{19}*$$

Good enough for practical use is the approximation (with reversed sign):

$$K' = \begin{pmatrix} 6 & -18 & 0 \\ 3 & 1 & -19 \end{pmatrix}. \tag{20}$$

In drawing crystals of the hexagonal system it is customary to turn the crystal 30° further clockwise than for other systems. This changes the clinographic matrix. It can be conveniently taken as

$$K_H = \begin{pmatrix} 758 & -963 & 0 \\ 110.7 & 52.7 & -1000\,c \end{pmatrix}. \tag{21}$$

If D is the two dimensional vector giving the direction of the projection of an edge we have:

$$D = K(E)_x. \tag{22}$$

But $(E)_x = M(E)_a$ where

$$D = KM(E)_a. \tag{23}$$

As an example we again take rhodonite

$$K'M = \begin{pmatrix} 6 & -18 & 0 \\ 3 & 1 & -19 \end{pmatrix} \begin{pmatrix} 1.016 & .0753 & 0 \\ 0 & .970 & 0 \\ -.345 & -.230 & .621 \end{pmatrix}$$

$$= \begin{pmatrix} 6.70 & -17.01 & 0 \\ 10.60 & 5.57 & 11.80 \end{pmatrix}$$

Whence, the edge, for instance, between $(\bar{2}\bar{2}1)$ and (100) which is

$$E_{100}^{\bar{2}\bar{2}1} = \begin{pmatrix} 0 \\ 1 \\ 2 \end{pmatrix}$$

is projected as

$$KM = \begin{pmatrix} 0 \\ 1 \\ 2 \end{pmatrix} = \begin{pmatrix} 6.70 & -17.01 & 0 \\ 10.60 & 5.57 & 11.8 \end{pmatrix} \begin{pmatrix} 0 \\ 1 \\ 2 \end{pmatrix} = \begin{pmatrix} -17.01 \\ 29.2 \end{pmatrix}.$$

Hence, in Fig. 3, we would lay out 17.01 units to the left of the origin and 29.2 units up. The edge projection is parallel to this line. It may be

* Here the bottom row $(18/\sqrt{370},\ 6/\sqrt{370},\ 1/\sqrt{37})$ has been omitted from the complete matrix K. The complete matrix is convenient for the computation of stereoscopic pairs of drawings of objects viewed from the clinographic angle. This subject will be presented in a later paper.

more convenient to compute angles from the vertical in terms of the tangents. As $\tan \delta = D_1/D_2$, see Fig. 3, if D_1/D_2 is positive S is measured

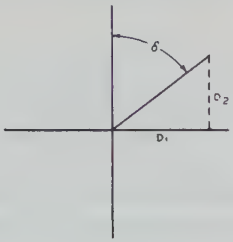

FIG. 3

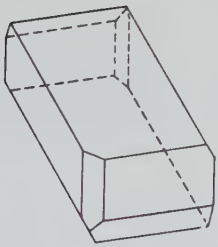

FIG. 3a. Rhodonite as drawn from matrix calculations.

clockwise from the vertical, counterclockwise if D_1/D_2 is negative. Slide rule computations are entirely satisfactory.

SUMMARY

(1) A vector $(V)_a$ on the a basis becomes $(V)_x = M(V)_a$ on the x basis.

(2) A vector can be normalized by dividing it by the square root of the sum of the squares of its components on the x basis.

(3) The cosine of the angle S between two unit vectors $(V)_x$ and $(W)_x$ is $\cos S = (\overline{V})_x(W)_x$.

(4) The vector $\begin{pmatrix} h \\ k \\ l \end{pmatrix}_A$ is perpendicular to the plane (hkl) and hence this plane has a normal on the x basis of:

$$(N_{hkl})_x = \overline{M}^{-1} \begin{pmatrix} h \\ k \\ l \end{pmatrix}_A$$

(5) The zone symbol $[mnp]$, derived from any two faces of the zone

by cross multiplication of the face indices, is a vector $\begin{pmatrix} m \\ n \\ p \end{pmatrix}_a$. It becomes on the x basis:

$$(V)_x = M \begin{pmatrix} m \\ n \\ p \end{pmatrix}_a .$$

(6) A clinographic projection of a crystal may be made by multiplying the matrix KM by the zone symbols of the crystal face pairs.

A CHART FOR MEASUREMENT OF INTERFERENCE FIGURES[1]

HORACE WINCHELL[2]

ABSTRACT

A simple but general chart has been developed for the solution of Mallard's formula and other relations used in the quantitative interpretation of interference figures produced by anisotropic crystals in convergent polarized light. This chart represents a general solution of the equations:

$$\frac{2D}{2} = K \sin \frac{2E}{2} = N_Y K \sin \frac{2V}{2} = NK \sin \frac{2H}{2}.$$

The chart can be used conveniently for certain types of orientation measurements as well as for the measurement of optic axial angles of biaxial crystals.

INTRODUCTION

Most mineralogists are familiar with the use of the petrographic microscope for measuring optical properties of crystalline materials. Two reference books commonly available in mineralogical libraries are Winchell (1937)[3] and Johannsen (1918), which cover the methods in some detail.

Several of the more convenient methods of measuring the optic axial angle 2V, or its equivalent in air 2E, or in water or other medium 2H, are based upon the use of a relationship known as Mallard's formula (Johannsen, 1918, art. 411). This formula is

$$D = K \sin E. \tag{1}$$

The quantity D is half the distance between the melatopes or points of emergence of the optic axes ("eyes") in a centered interference figure produced by a crystal section normal to the acute bisectrix. D is measured in terms of the linear units of the scale of an eyepiece fitted with a micrometer scale; K is a constant depending upon the optical system and the spacing of the scale divisions in the micrometer eyepiece; and E is half the apparent optic angle in air.

The relation between E, V, and N_Y is given by the following formula:

$$\sin E = N_Y \sin V. \tag{2}$$

In equation (2), E is as defined above; N_Y is the intermediate index of refraction of the crystal; and V is half the true angle between the optic axes.

[1] Contribution of the Research Engineering Division of the Hamilton Watch Company, Lancaster, Pennsylvania.

[2] Formerly Research Crystallographer, Hamilton Watch Company, Lancaster, Pennsylvania; now at Department of Geology, Yale University, New Haven, Connecticut.

[3] Bibliographic references are identified by the author's name and the year of publication. See bibliography for complete references.

Equations (1) and (2) may be combined as follows:

$$D = K \sin E = KN_Y \sin V. \tag{3}$$

Rarely, the apparent optic angle 2H, in some other medium than air or the crystal may be desired. In this case the index of refraction of the medium will be denoted by N:

$$D = K \sin E = KN \sin H. \tag{4}$$

However, it is conventional to express these angles in terms of 2E, 2V, and 2H; likewise the distance between the two melatopes 2D, is the quantity actually measured, rather than the distance D, of one melatope from the center of the field. Therefore equations (1) to (4) will be more useful for most purposes if expressed in terms of 2D, 2H, and 2V:

$$\frac{2D}{2} = K \sin \frac{2E}{2} = KN \sin \frac{2H}{2} = KN_Y \sin \frac{2V}{2}. \tag{5}$$

The first part of equation (5) has been expressed graphically in the Schwartzmann optic angle scales (Winchell, 1937, p. 188; Johannsen, 1918, art. 413) which relate 2D and 2E. These scales are on many slide rules: D or 2D may be represented by the A scale of the slide rule; 2E, graduated in terms of E rather than of 2E, may be represented by the S scale of the slide rule. Each optical system requires its own characteristic setting of the slide rule (or of the Schwartzmann scales) to determine E or 2E from D or 2D. Two settings of the slide rule are required to convert the observed value, 2D, into the true optic angle 2V.

The Chart

Figure 1 is a logarithmic chart showing the relations expressed in equations (5). The 2D, K, and N scales are ordinary logarithmic scales similar to those used for multiplication on a slide rule; the 2E scale is a logarithmic sine scale divided like the S scale of a slide rule, but numbered differently. Like Schwartzmann's scales, this chart must be calibrated for the particular microscope and lenses used. Unlike the Schwartzmann scales, Fig. 1 may be *permanently* calibrated for *several* optical systems in one or more microscopes. One copy of this chart therefore suffices for use with all combinations of lenses in a given microscope, and may be calibrated therefor; similarly, one large copy of the chart would serve a laboratory equipped with several microscopes. This chart also differs from Schwartzmann's scales in showing 2V and 2H as well as 2E.

Calibration and Use of the Chart

The method of use of Fig. 1 is indicated briefly in the key at the top. The calibration is analogous to that used for setting the Schwartzmann

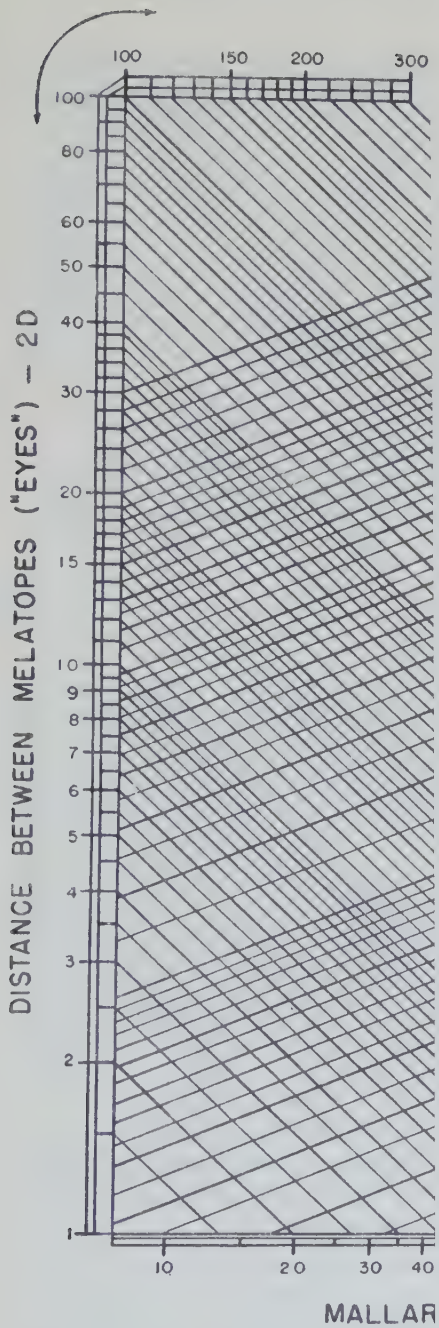

FIG. 1. Chart of $2D/2 = K \sin (2E/2) = N_Y K$
Measurement of optic axial angle from acut
1. Calibrate by drawing vertical line th
2. Measure 2D in interference figure und
3. Follow lines as shown in key.

axial angle scales. The interference figure of an oriented section of a mineral of known optic angle is carefully measured and the result is used for calibrating the chart. A micrometer eyepiece is used to measure the distance 2D, between the melatopes. Sodium light should be used if possible, whenever an interference figure is to be observed and measured, for the sharpness of the isogyres is usually improved by monochromatic light, and nearly all published descriptions of natural and artificial crystalline compounds give optical properties measured in sodium light.

An example will illustrate the calibration and use of the chart. The following data were obtained for an oriented section of aragonite:

Microscope:	Spencer No. 37, Ser. No. 154974
Objective:	Spencer achromatic, 4-mm. dry
Eyepiece:	Spencer Huygenian, 10×
Micrometer:	20 divisions per millimeter
Bertrand lens:	Focused at 5.2

Diameter of field	58 (observed)
2D	18.5 (observed)
2E	31° (Winchell, 1933, p. 79)

These data were applied to the calibration of the chart as illustrated in Fig. 2. The sloping line from $2D = 18.5$, and the sloping line from $2E = 31°$ intersect at a point directly above $K = 34.5$ on the horizontal scale. Through this point of intersection a vertical *calibration line* was drawn, extending from the K-scale upward to a terminus corresponding to $2D = 58$, the diameter of the interference figure with this setup and hence the largest 2D that can be measured with it. This line was labelled to correspond with the optical system concerned. It is the calibration line for that system. By this construction, Mallard's constant K has been determined for the system, and that value could be used in equation (5) for future determinations of 2E, 2V, and 2H, in terms of 2D and the appropriate refractive index. Conversely, if K is determined by any other means, the position of the calibration line is thereby also determined.

Assuming that the chart has been calibrated for the 4-mm. objective and the 10× micrometer eyepiece, as just described for Fig. 2, it is now ready for use for the determination of 2E and 2V, and for an additional purpose which will be described below. An interference figure from a section which is oriented with the acute bisectrix nearly normal to it may now be used to measure 2E and 2V. For example, if the measured distance 2D is 45 units in the micrometer eyepiece scale, the chart is entered at $2D = 45$; a line is followed down and to the right to the calibration line, and from that point a new line is followed up and to the right to the side of the chart where 2E is read: $2E = 80°$. However, if an ap-

proximate estimate of the index of refraction of the material gave $N_Y = 1.60$, then instead of reading $2E = 80°$, the line may be followed up and to the right from the calibration line to the 1.60 vertical line, and thence down and to the right to $2V = 47°$. In most cases, a small error in the estimate of N_Y will not greatly affect the value of 2V; therefore

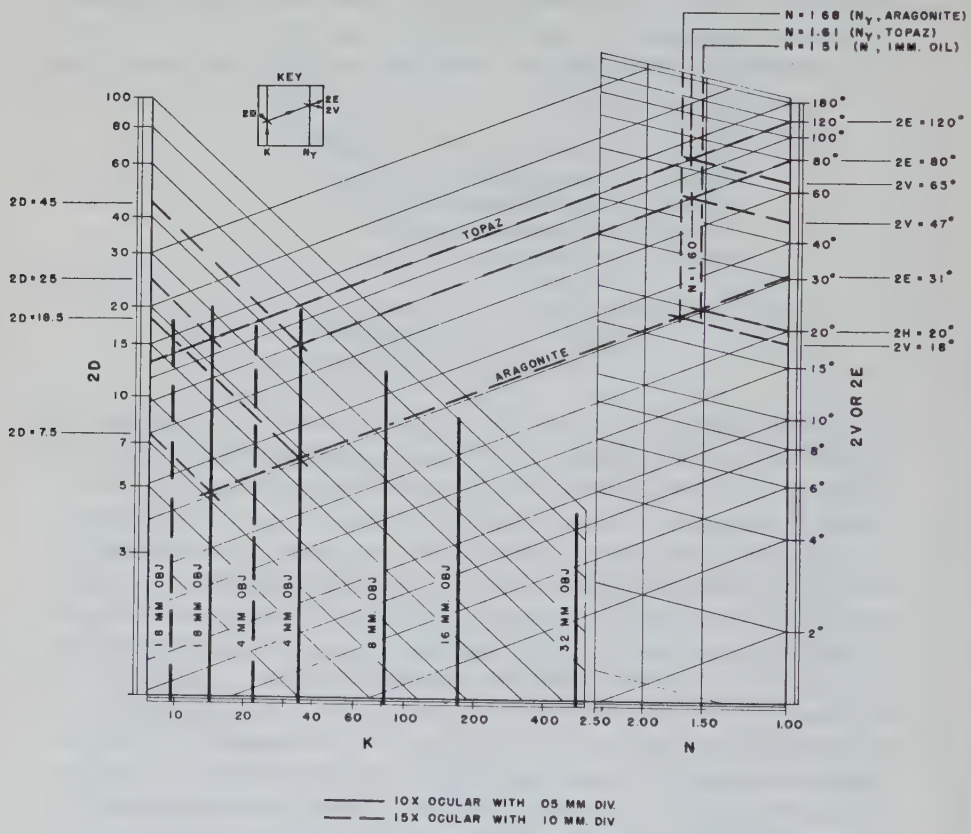

FIG. 2. Chart like Fig. 1, calibrated for use with several optical systems on Spencer petrographic microscope, serial number 154974.

a closely-graduated refractive-index scale is neither necessary nor desirable.

A further example may be taken from the calibration of the chart for a 1.8-mm. oil-immersion objective. The chart was calibrated for this objective using topaz, and the result was checked using aragonite. The following data were assembled:

Microscope: Spencer No. 37, Ser. No. 154974
Objective: Spencer achromatic, 1.8-mm., oil imm.
Eyepiece: Spencer Huygenian, 10×
Micrometer: 20 divisions per millimeter
Bertrand lens: Focused at 7.0

Diameter of field 32 (observed)

	Topaz	Aragonite
N_Y (measured)	1.613	
2V (see text)	65°	
2E		31°
2D (measured)	22.5	about 7 or 8

The optic angle of topaz varies considerably with variations in composition, but two considerations justify its use in this instance. First, the apparent optic angle 2E is about 120°; this value falls in the greatly compressed portion of the 2E scale, so that a considerable error in the numerical value of 2E (or of 2V) will introduce only a small error in the position of the corresponding point on the scale. Second, the intermediate index of refraction of the specimen had been previously measured. This value, N_Y, was 1.613; comparison with published data (Winchell, 1933, p. 199, Fig. 118) shows that topaz with $N_Y = 1.613$ contains about 5 per cent of the hydroxyl end-member of the topaz series, and that for this composition $2V = 65°$.

Since 2E is unknown, 2V and N_Y are used to obtain the left-sloping line for calibration of the chart: starting at $2V = 65°$ follow up and to the left to the vertical line for $N_Y = 1.613$, and from that point down and to the left to the intersection with the right-sloping line from $2D = 22.5$. Through the point thus located, the vertical calibration line is drawn from the K-scale (at $K = 14$) to the point corresponding with the diameter of the field of view. As a check, the observation of the interference figure of aragonite gave 2D = between 7 and 8; using the calibration line just determined, 2E is therefore between 29 and 33 degrees, which is good agreement with the known value of 31° for aragonite.

Instead of 2V or 2E, 2H may be read from the chart if the index of refraction of the immersion oil is known. For example, the oil used with the 1.8-mm. objective described above has an index of 1.515. The optic angle in this oil would be designated 2H, and is obtained by a procedure similar to that described above for 2V, except that the index of the oil, $N = 1.515$, is used instead of the index of the crystal, N_Y. Thus for aragonite, $2H = 20°$, $2V = 18°$, $2E = 31°$. 2H in water ($N = 1.33$) would be about 24.

By a similar process the chart may be calibrated for other optical systems. This has been done as just described for our oil-immersion 1.8-mm. objective, and for our dry 4-, 8-, 16-, and 32-mm. objectives with the 10× micrometer eyepiece, and for the 1.8-mm. and the 4-mm. objectives with a 15× Ramsden eyepiece, fitted with a scale having 10 divisions per millimeter. All these calibration lines are shown in Fig. 2.

A further use for this chart (the one for which the chart was originally developed in the laboratories of the Hamilton Watch Company) is the measurement of an orientation angle, R; this angle is defined for present purposes as the true angle between the optic axis of a uniaxial crystal plate (or any other optically recognizable direction in an anisotropic crystal plate) and the normal to the plane of the section. Actually, of course, R is measured between the optical crystal direction and the optical axis of the microscope. For example, synthetic corundum jewel bearings may be studied by this means (Winchell, 1944), although other methods give more complete data. The jewel bearing often consists of a round, flat disc of corundum, polished all over, with a polished hole through its center. The relation of this hole, normal to the plane of the disc, to the crystallographic axes of the corundum, is important in the study of the processing and wearing qualities of the jewel. Using sodium light, we obtain an interference figure, measure the radial distance D, from the center of the figure to the melatope (in this case, the black cross corresponding to the optic axis of the corundum). We then enter the chart at 2D as for an optic angle determination, follow the lines down to the calibration line, then up to the appropriate refractive index line ($N_o = 1.77$), and finally down to the value of 2R; from 2R, R is easily obtained. Great advantage is obtained in using monochromatic light for this operation, since it is thereby possible to use the isochromatic curves to locate with accuracy the center of the flash figure in sections in which R is very large and the melatope is outside the field of view. From the orientation of the flash figure we obtain the complement of R, and hence the angle R itself.

A similar technique has been tried successfully, but never actually put to use by the writer, for determining the orientation of a biaxial crystal. In this case, a bisectrix and an optic axis were visible in the interference figure, and by noting for each the polar angle R and the azimuth V, which can be measured directly with the graduations on the periphery of the rotating stage, it was possible to construct in stereographic projection the complete orientation of the optical indicatrix with respect to the thin section. This included the determination of the value of 2V and the identification of the bisectrix visible in the field of view. It is probable that this method would fail if the normal to the section

makes too great an angle with all three of the optic symmetry planes, and possibly also under certain other conditions, unless an objective of extremely high aperture is used. The 1.8-mm. oil-immersion objective whose calibration is shown in Fig. 2 would always produce an interference figure including at least one of the principal optical directions, X, Y, or Z, and usually also one of the optic axes (melatopes) provided that the refractive index of the specimen is low enough. Since this application would probably be rare, a complete description is hardly justified here. One of its uses would be the determination of optic orientation in laboratories where a universal stage is not available.

Discussion

A minor refinement on the use of Fig. 1 for orientation measurements would be accomplished by substituting a scale of E for scale of 2E. In so doing, each number is replaced by one which is half as large. Similarly, the scale of 2D could be replaced with a scale of D. However, the latter change would be unnecessary, since dividing the numbers by 2 would have the same effect as bodily shifting the scale upward a distance equal to the distance between any pair of numbers having a ratio of 1:2 (e.g., 10 and 20, 15 and 30, etc.). Shifting the scale requires a corresponding shift in the position of the K-scale, however. A shifted scale requires recalibration of the chart.

The chart could of course be made perfectly general in scope by drawing a family of vertical lines to represent the K-scale or Mallard's constant. Then the procedure for use would be to enter the chart at 2D and K, follow corresponding lines to their intersection, then from that intersection follow the proper line up and to the right as described above. That procedure would always involve the use of the numerical value of K, rather than a relatively isolated and easily-located calibration line. Since only a small number of fixed values of K will ordinarily be used in connection with the chart it seems better to retain it as in Fig. 1, without the complete family of vertical lines.

It should be noted that if the 2D-scale, which in its present form covers about $2\frac{1}{2}$ logarithmic cycles, should prove inadequate to cover the ranges of values necessary, this scale may be multiplied or divided by any desired factor. The K-scale should then be changed by the same factor. For example, in using a filar micrometer reading in millimeters and fractions rather than units of 0.1 or 0.05 millimeter, a more suitable range of values for 2D might be from 0.01 to 3.00 instead of from 1 to 300.

The K-scale would be renumbered accordingly, and would then read from 0.10 to 5.00 instead of from 10 to 500.

Summary

Figure 1 is an expansion and development of the principles of the Schwartzmann optic axial angle scales; this chart facilitates the prompt and easy solution of Mallard's formula and the laws of refraction, so as to give the optic axial angle in air or any medium (including the crystal itself), from a simple measurement of the distance between the melatopes or "eyes" in an acute bisectrix interference figure. The specific advantages of the chart method over the Schwartzmann scales are (1) no need to cut out, trace, or otherwise reproduce the logarithmic Schwartzmann scales to permit calibration, or to find and calibrate a slide rule containing logarithmic and logarithmic sine scales: the chart may be calibrated by drawing a single straight line through a single calibration point; (2) only one chart is needed for permanent reference purposes, and the calibration of the chart may permanently include data for more than one optical system; (3) the chart solves the problem for 2V and 2H as well as for 2E, thus eliminating a second setting for the slide rule method, or a separate calculation of 2V or 2H after obtaining 2E by the Schwartzmann method. Application of these specific advantages facilitates certain orientation measurements that otherwise would normally be made with a universal stage, or at considerably more labor with interference figures, Schwartzmann scales, and auxiliary calculations.

Acknowledgments

The chart herein described was developed in connection with investigations of the relation between orientation and processing efficiency in corundum boules, and between orientation and durability of corundum jewel bearings, in the laboratories of the Hamilton Watch Company. The writer is particularly indebted to Mr. B. L. Hummel of the Engineering Records Section for suggestions and aid in preparing the finished drawings, and for various reproductions thereof at several sizes.

References

Johannsen, Albert (1918), *Manual of Petrographic Methods*, Sixth Edition, New York.

Winchell, A. N. (1937), *Elements of Optical Mineralogy, Part I: Principles and Methods*, Fifth Edition, New York.

———, (1933), *Elements of Optical Mineralogy, Part II: Descriptions of Minerals*, Third Edition, New York.

Winchell, Horace (1944), Orientation of synthetic corundum for jewel bearings: *Am. Mineral.*, **29**, 399–414.

PETALITE AND AMBLYGONITE FROM KARIBIB, SOUTH WEST AFRICA*

H. J. Nel, *Geological Survey, Pretoria, South Africa.*

Abstract

A detailed description of the physical and chemical properties of petalite [$LiAl(Si_2O_5)_2$] and amblygonite [$LiAlPO_4(OH,F)$] from the Karibib district of South West Africa is given here for the first time. Both these minerals constitute potential lithium ores in this area.

Introduction

Petalite and amblygonite are known in Southern Africa only from the lepidolite deposits in the Karibib district, South West Africa. The lithium minerals occur in pegmatite bodies which are genetically related to the Salem granite. In this area both the granite and the pegmatite invade the rocks of the Damara System which consists of metamorphosed sediments, now represented by quartzite, marble and biotite schist.

In 1940 C. M. Schwellnus and H. D. le Roex† reported on the lithium mineral deposits of the Karibib district. They found that lepidolite, sometimes containing up to 6% Li_2O, is the most common lithium mineral. Amblygonite and petalite with approximately 9% Li_2O and 4% Li_2O respectively, also constitute potential lithium ores.

In discussing the mode of occurrence of these minerals, they state that: "The lithium-bearing minerals all occur in quartz blows. . . . Amblygonite essentially occurs as completely isolated blebs within the quartzose part of the pegmatite bodies. The individual blebs vary in size from less than an inch to a few feet across and have been found in places to yield as much as five tons of massive amblygonite. Unfortunately the blebs are very erratic both in size and distribution . . . ."

"Petalite occurs in much lesser quantities than the lepidolite, but certainly in much greater abundance than the amblygonite. It is usually confined to the quartz and occurs mostly in close proximity to amblygonite. Huge massive blocks of this material (i.e. the petalite) can be seen in most of the deposits."

Petalite

A specimen of petalite from the farm Kaliombo 42, approximately 20 miles east of the village of Karibib, South West Africa, was made avail-

* Published by permission of the Honourable the Minister of Mines.

† Departmental report.

able for study through the courtesy of Mr. H. D. le Roex, formerly of the Geological Survey.

The petalite is massive, gray-white in colour and mainly translucent. The cleavage (001) is well developed, while there is sometimes the tendency to split along (201) when struck with a hammer. On (001) the lustre is pearly, otherwise it is usually vitreous. The mineral crystallises in the monoclinic system.

The specific gravity, determined by suspension of pure fragments of petalite in a solution of bromoform and alcohol, is $G_4^{14} = 2.422 \pm .005$. The hardness on the (001) cleavage plane is ± 6.5.

According to most textbooks on mineralogy, petalite emits a blue "phosphorescent" light when gently heated. Both finely powdered petalite and a single piece of about half a cubic inch were at first gently and later more strongly heated on a hot plate: in no case was any thermoluminescent effect observed. Exposing the unheated and heated petalite to sunlight and to radiation from a quartz mercury lamp failed to produce any phosphorescence. Petalite from Sweden also gave negative results under the same conditions.

A fine-grained isotropic white mineral, probably an alteration product, is sparsely distributed through the petalite. This mineral, which is both too fine grained and too sparingly present to permit identification by ordinary chemical or microscopic methods, is probably the cause of the observed translucence of the petalite. It may be of interest to mention here that Quensel (1) records montmorillonite as an alteration product of petalite from the Varuträsk pegmatite, Sweden.

In thin section cut parallel to (001), the massive petalite is seen to be composed of irregularly shaped individuals differing very slightly in optic orientation, so that extinction is not obtained simultaneously on all these components. From sections cut approximately parallel to (100) and (010) it could be established that these components, which are roughly lath-shaped, have their longest direction approximately parallel to the crystallographic axis *c*, and their shortest direction approximately parallel to *b*.

Optical Properties

The refractive indices of the petalite (and that of the amblygonite described in this paper) were determined according to a single variation method. The mineral grains were brought to the desired orientation on a universal stage (2, p. 18) and the refractive indices matched at room temperature with those of mixtures of suitable immersion liquids of high dispersion, by adjusting the wavelength of the monochromator. The refractive indices of the petalite are given in Table 1.

TABLE 1

	F (486 mμ)	D (589 mμ)	C (656 mμ)
α	1.512	1.507	1.505
β	1.517	1.512	1.510
γ	1.523	1.518	1.516

(all values correct to ±.001)

Birefringence $(\gamma-\alpha)=.011$
Dispersion $(\beta_F-\beta_C)=.007$
$2V_\gamma$ (calculated) $=84°$
$2V_\gamma$ (observed) $=82°\pm1°$
Optic axial plane $\perp(010)$
Extinction $X/a=2°\pm2°$.

There is no noticeable dispersion of the optic axes in petalite. In thin section of standard thickness examined conoscopically and on the universal stage by monochromatic light of different wavelengths, no dispersion could be observed. The value of $2V\gamma$ is constant, within experimental error, for light from 480–650 mμ. The petalite shows marked conical refraction in thin section of standard thickness.

Chemical Properties

The spectrographic and chemical analyses of the petalite listed below were done on specially selected fragments which were examined microscopically and found to be free from impurities.

TABLE 2. CHEMICAL ANALYSIS

a.		*b.*	*c.*		*d.*			
SiO_2	77.18	1.2850	Si	1.2850	15.90	Si	15.90	(16)
Al_2O_3	16.04	0.1573	Al	0.3146	3.89	Al	3.99	(4)
Fe_2O_3	0.64	0.0040	Fe	0.0080	0.10			
CaO	0.22	0.0039	Ca	0.0039	0.05			
MgO	0.26	0.0064	Mg	0.0064	0.08	Li	4.20	(4)
Na_2O	1.14	0.0184	Na	0.0368	0.46			
Li_2O	4.36	0.1459	Li	0.2918	3.61			
H_2O+	0.40	0.0233	H	0.0466	0.58	H	0.58	
H_2O-	0.02		O	3.2518	40.42	O	40.24	(40)
Total	100.26							

a. Chemical analysis by C. J. Liebenberg.
b. Molecular proportions.
c. Atomic proportions.
d. Calculation of the unit cell formula from the relationship.

Qualitative Spectrographic Analysis

Present Li, Al, Si, *Mg, Na, Ca, Fe.*
Trace B, F, Ga, Mn, Cr.
Absent K, Ge, Tl, Sr, Ba, Cs, Be, Ti, Rb.
Analyst: *B. Wasserstein.*

$$\text{Number of ions of each element in the unit cell} = \frac{\text{Unit cell volume} \times \text{Avogadro's Number} \times \text{Atomic Ratio} \times \text{Density}}{\text{Sum total of the chemical analysis}}.$$

The unit cell volume (*abc* sin $\beta = 844.8$ cu. Å) was obtained from the unit cell dimensions of petalite from Elba, given by Gossner and Mussgnug (3, p. 64) viz:

a	11.77 Å
b	5.13 Å
c	15.17 Å
B	112°44′

Assuming that these dimensions are reported in Siegbahn units, a value of $(6.0597 \pm 0.0016) \times 10^{23}$ is used for Avogadro's number (4, p. 110). The density of the petalite is 2.422.

The unit cell formula of petalite may therefore be expressed as $Li_4Al_4Si_{16}O_{40}$, that is, the unit cell contains four molecules with the composition $LiAl(Si_2O_5)_2$, which agrees with the results first obtained by Gossner and Mussgnug. As can be seen from Table 2, column *d*, the amount of water present in the unit cells is too low to be considered in the formula. The ratio of Li to Na is 7.93:1.

In conclusion it may therefore be stated that the petalite from Karibib, South West Africa, does not differ markedly in physical and chemical properties from petalite reported from other parts of the world.

Amblygonite

The massive amblygonite (Geological Survey Museum No. 6614) has a well developed cleavage, and is white with a bluish tinge in patches where the mineral is perfectly fresh. The lustre is vitreous to greasy. Polysynthetic twinning, frequently reported in amblygonite, is sporadically developed in the numerous thin sections examined. Amblygonite crystallises in the triclinic system.

The specific gravity of the amblygonite was determined on carefully selected fragments by suspension and gave $G_4^{14} = 3.085 \pm .005$. The hardness is ± 5.5. Finely powdered amblygonite does not readily dissolve on boiling in either concentrated or 1:1 HCl, H_2SO_4 or HNO_3. A sufficient amount of the mineral does, however, go into solution with boiling concentrated HNO_3 to give the phosphate test with ammonium molybdate.

Optical Properties

In thin section it could be established that two cleavage directions (100) and $(0\bar{1}1)$* are represented, with the former direction more prominently developed. By means of these cleavages the optic orientation of the amblygonite could be established on the universal stage. This orientation (7, p. 42) is given in Table 3, together with the position of

TABLE 3

	ϕ	ρ
X	19°	69°
Y	−78°	72°
Z	156°	28°
100	110°	90°
$0\bar{1}1$	162°	24°
$100 \wedge 0\bar{1}1$	75°	

the two cleavages already mentioned. The positions of X, Y and Z are stated correct to 2°.

Further optical data are given in Table 4.

TABLE 4

	F (486 mμ)	D (589 mμ)	C (656 mμ)
α	1.599	1.594	1.592
β	1.613	1.608	1.606
γ	1.621	1.616	1.614

(all values correct to ±.001)

Birefringence $(\gamma-\alpha) = .022$
Dispersion $(\beta_F-\beta_c) = .007$
$2V\alpha$ (calculated) $= 74°$
$2V\alpha$ (measured) $= 75° \pm 2°$
No dispersion of the optic axes could be observed.

Chemical Properties

The spectrographic and chemical analyses of the amblygonite were done on material free from impurities.

* Richmond and Wolfe (5, p. 41) recently proposed a new crystallographic orientation, based on x-ray studies, for amblygonite. Transformation formula: Dana to Richmond and Wolfe 001/011/100. This new orientation is used in this paper.

Qualitative Spectrographic Analysis

Present Li, Al, P, Na.
Trace Ga, Ca, Mg, Fe, Mn, K.
Absent Ba, Rb, Cs, Tl, Ti, B, Be, V, Ni, Co, Sr, Si, Rare earths.

Analyst: *B. Wasserstein*

Table 5. Chemical Analysis

a.		*b.*	*c.*		*d.*		
Al_2O_3	35.19	0.3452	Al	0.6904	2.06 Al	2.06	(2)
P_2O_5	47.54	0.3347	P	0.6694	2.00 P	2.00	(2)
Li_2O	9.65	0.3230	Li	0.6460	1.93		
Na_2O	0.43	0.0069	Na	0.0138	0.04 Li	2.00	(2)
K_2O	0.10	0.0011	K	0.0022	0.01		
MgO	0.33	0.0082	Mg	0.0082	0.02		
F	5.40	0.2842	F	0.2842	0.85 OH+F	1.94	(2)
H_2O+	3.26	0.1832	H	0.3664	1.09		
H_2O-	0.04						
	101.94		O−F	2.9473	8.80 O*	7.71	(8)
Less O for F	2.27						
	99.67						

*After an equivalent amount of O has been subtracted for F.

a. Chemical analysis by C. J. Liebenberg. (Fluorine determination by P. J. Hamersma).

b. Molecular proportions.

c. Atomic proportions.

d. Calculation of the unit cell formula, using a unit cell volume of 159.11 cu. Å (5, p. 47) and a specific gravity of 3.085 as determined on the Karibib amblygonite. The calculation is made on the same basis as that of the petalite formula.

The unit cell formula of the amblygonite is therefore $2[LiAlPO_4(OH,F)]$ which is the same as that obtained by Richmond and Gonyer (5, p. 47) on amblygonite from Hebron, Maine. The ratio of OH to F is approximately 1.30:1.

The composition of the amblygonite may also be expressed in terms of the end members of the series, namely, 44% amblygonite ($LiAlPO_4F$) and 56% montebrasite ($LiAlPO_4OH$). There is a reasonably good agreement between the refractive indices of the Karibib amblygonite and the values given by Winchell (6, p. 248) in his diagram for the amblygonite-montebrasite series, for amblygonite of the composition stated above. Winchell does not claim his diagram to be highly accurate, and since its publication in 1926 there is still the need for chemical analyses,

coupled with physical data, of members of the amblygonite-montebrasite series.

Acknowledgments

The writer wishes to thank Mr. C. J. Liebenberg and Dr. P. J. Hamersma of the Division of Chemical Services, Pretoria, for the chemical analyses. The qualitative spectrographic analyses by Dr. B. Wasserstein of the Geological Survey are also gratefully acknowledged. Prof. B. V. Lombaard of the University of Pretoria critically reviewed the manuscript; the writer is indebted to him for many useful suggestions.

References

1. Quensel, P., Minerals of the Varuträsk pegmatite. IV. Petalite and its alteration product, montmorillonite: *Geol. Fören. Stockh. Förh.*, **59,** 150 (1937).
2. Emmons, R. C., The Universal Stage: *Geol. Soc. Am., Memoir* **8,** (1943).
3. Gossner, B., and Mussgnug, F., Über die strukturelle und molekulare Einheit von Petalit: *Zeits. Kris.* **74,** 62 (1930).
4. Schlecht W. G., Calculation of density from x-ray data: *Am. Mineral.*, **29,** 108 (1944).
5. Palache, C., Richmond, W. E., and Wolfe, C. W., On amblygonite: *Am. Mineral.*, **28,** 39. (1943).
6. Winchell, A. N., Relationship between properties and composition in the amblygonite-montebrasite series: *Am. Mineral.*, **11,** 248 (1926).
7. Palache, C., Berman, H., and Frondel, C., *Dana's System of Mineralogy.* 7th Ed. Vol. **1,** J. Wiley and Sons, N. Y., (1944).

SECONDARY DAUPHINÉ TWINNING IN QUARTZ PRODUCED BY SAWING. IRRADIATION OF TWINNED QUARTZ

CLIFFORD FRONDEL,
*Harvard University, Cambridge, Massachusetts.**

ABSTRACT

Instances are described in which Dauphiné twinning has been formed artificially in quartz by sawing. The secondary twinning occurs as a very thin surface layer, usually on one side of the saw cut only, and seems to have been produced by frictional heat developed at the cutting edge of the saw blade. The twinning often is restricted to particular growth zones in the quartz. The tendency to twin is related to the tendency of quartz to become smoky in color when irradiated with x-rays, easily twinned quartz being relatively little affected.

The boundaries of some natural Dauphiné twins in quartz coincide with natural smoky color zones. In these specimens the original boundary of the twin is returned more or less exactly when the crystals are re-inverted at 573° C., and a differential smoky coloration opposite to that existing initially is affected across the original twin boundary by radiation. Brazil and natural Dauphiné twins of colorless quartz sometimes also may be differentially pigmented by radiation, but Dauphiné twins produced artificially in originally untwinned quartz are not so affected.

Inspectors in the sawing department of a company manufacturing quartz oscillator-plates recently drew attention to sawn BT (−49°) wafers that, when etched, revealed the pattern of Dauphiné (electrical) twinning on one side of the wafer only. The wafers were 0.045″ thick and ranged up to several inches in length. Up to 5 per cent or so of the daily production of wafers has been found twinned in this way but the usual percentage is about 0.5.[1] The one-sidedness of the twinning was explained on the assumption that the wafers chanced to be cut more or less tangentially through the boundary of a Dauphiné twin originally present in the raw crystal.

This interpretation proved to be erroneous for most instances, at least, when it was observed that successive wafers sawed from the same raw crystal were all twinned on one side of the wafer only, and on the same side relative to the saw blade. In some instances, as many as seven or eight successive wafers from the same raw crystal were twinned in this way. Instances also were found in which Dauphiné twin patterns were present on both sides of the wafer but not in coincidence, and when these wafers were lapped down 0.005 inch or so on each side and then re-etched the twinning was found to have been removed. In general,

* Contribution from the Department of Mineralogy and Petrography, Harvard University, No. 271.

[1] The total number of rough quartz wafers produced during 1941–1945 in the United States is roughly estimated at 200,000,000 and their cost, including that of raw material and processing, at about $100,000,000.

the twinning extends to a depth of less than 0.010 inch and usually to only a few thousandths of an inch or so, although the surface area of the twinning may range up to several square inches. The twinning thus is only in a thin surface layer, and the geometry of its occurrence is such as to negate the explanation first given. It evidently is of secondary

FIG. 1 FIG. 2

FIGS. 1 and 2. Secondary Dauphiné twinning in BT quartz wafers produced by sawing. The mounting surface seen edgewise at the bottom is $(11\bar{2}0)$. The twinning is revealed by examining the etched surface in reflected light.

origin and presumably was formed during the sawing operation. Twinned wafers of this type can be salvaged once the nature of the effect is recognized.

The twinning characteristically appears as irregular areas composed of elongated bands or stripes which may interconnect in part and then have a coarse graphic-like pattern (Figs. 1 and 2). The elongated bands usually are perpendicular to the mounting surface, $(11\bar{2}0)$. Sometimes the bands turn through an angle, with the bent part parallel to the trace of rhom-

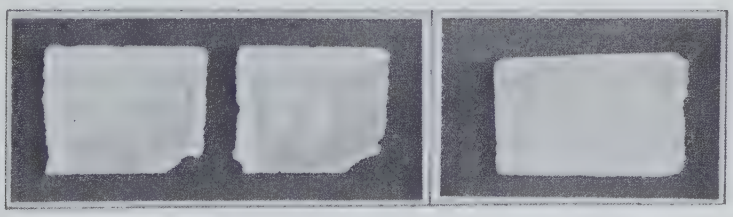

FIG. 3 FIG. 4

FIG. 3. Two successive wafers cut from the same raw crystal showing a blotchy type of secondary twinning. A narrow band of natural Dauphiné twinning appears on the left-hand edge of the wafers.

FIG. 4. A narrow band of secondary twinning following a smoky color zone in the quartz. A small patch of natural Dauphiné twinning appears in the upper left corner.

bohedral or prism planes on the plane of the saw cut. The arrangement of the bands is determined by growth zones in the quartz. In other instances, the twinning appears as a number of small irregular patches grouped together into a blotchy pattern (Fig. 3). Some examples are hardly more than surface films and resemble bruise marks. Surface twinning actually may be more common than appears, since the twinned layer probably has to be over about 0.0005 inch thick before it can be demonstrated by the etch pit method. There is not a close resemblance to ordinary electrical twinning, although its identity as such is proven by the method of Willard[2] involving an oriented reflection of a beam of light from the etched surface.

One very interesting feature observed is that the secondary twinning sometimes is confined to smoky zones in the quartz and terminates sharply against the colorless quartz at the zone boundary (Fig. 5*a* and

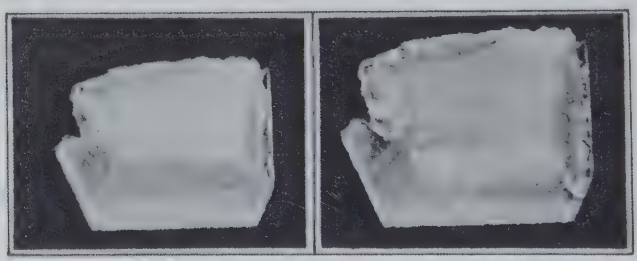

FIG. 5. The right-hand figure shows a wafer in which the secondary twinning is restricted to a smoky color zone in the quartz. The left-hand figure shows the same wafer in a position such that the twinned area does not reflect.

5*b*). In other even more remarkable examples the twinning forms very narrow straight-sided bands or lines which on close examination are found to run along thin smoky growth bands in the quartz (Fig. 4). It is commonly found that if a batch of twinned wafers randomly accumulated by plant inspectors at the end of a day's work is examined, most of them can be matched together and have come from relatively few raw crystals. This suggests that certain raw quartz crystals are much more susceptible to secondary twinning than others. Different parts of individual raw crystals also have an unequal tendency to twin, as shown by the banded arrangement of the twinning and by the color zoning effect.

Many specimens of quartz, although not all, readily develop secondary Dauphiné twinning[3] not only by inversion at 573° but also by rapid

[2] Willard, G. W., Use of the etch technique for determining orientation and twinning in quartz crystals: *Bell Syst. Tech. J.*, **23**, 11 (1944).

[3] Frondel, C., Secondary Dauphiné twinning in quartz: *Am. Mineral.*, **30**, 447–460 (1945).

cooling from temperatures between 200° and 570°, and by high local pressure at room temperature and higher. In the present instance the twinning seems to have been caused by frictional heat developed at the cutting edge of the saw blade. The existence of high local temperatures during sawing is evidenced by the occurrence of sparking and of a bright glow along the arc of contact of the blade with the quartz. The glow may be due in part to triboluminescence. It is generally considered that the safe upper limit to sawing speed is set by the appearance of this glow; higher speeds give rise to undue damage to the surface of the wafer. Local heating may be further increased in the case of dull blades or blades in which the edge bead is small or lacking on one side.

Excessive blade pressure and an inadequate or interrupted supply of liquid coolant to the blade during operation are added factors. Efforts to deliberately produce secondary twinning during sawing by introducing the conditions mentioned above have not succeeded. Very heavy blade pressure, about three to five times the eight pounds per linear inch of cutting surface ordinarily practiced, with a dull blade and a much reduced supply of liquid coolant is found, however, to generate thermal strains sufficiently powerful to explosively shatter sections 0.25 inch thick into small jagged fragments.

The ease with which secondary twinning can be introduced into quartz lends credence to reports, which the writer has not been able to verify at first hand, that oscillator-plates occasionally become Dauphiné twinned during machine lapping. The development of twinning in this case presumably would be facilitated by an inadequate supply of lapping vehicle and abrasive, thus causing the lap to run hot, and by heavy pressure on the top lapping plate.[4] In even a badly abused machine lap, however, the temperature rises only to the neighborhood of 100° C or so, and the pressure on the crystals, which ordinarily is of the order of 1 to 4 pounds per square inch, can hardly exceed about 20 pounds and still leave the lap able to operate. Still, the nature of the lapping operation itself may be such that this degree of temperature and pressure are momentarily exceeded on a particular plate or part thereof. Information also has been received that Dauphiné twinning sometimes is formed locally when supporting wires are soldered to the surface of a metal-

---

Zinserling, E. V., Quartz twinning control under alpha-beta inversion: *Compt. Rend. Acad. Sci. URSS.*, **33,** 365 (1941).

Zinserling, E. V., Quartz colouring as dependent on its twinning capacity under alpha-beta conversion: *ibid.*, **33,** 368 (1941).

Zinserling, E. V., and Laemmlein, G. G., Conversion of a negative quartz rhombohedron into a positive one as a result of alpha-beta transformation: *ibid.*, **33,** 419 (1941).

[4] The machine lapping techniques used in the quartz oscillator-plate industry have been described by W. Parrish: *Am. Mineral.*, **30,** 389–415 (1945).

coated quartz plate by a tiny jet of hot air—the temperature of the jet purposely being kept well below 573° to avoid inversion—and also when the metal coating on a plate is divided into separate areas, as in certain types of harmonic resonators, by locally vaporizing the metal in a pin point arc.

Relation of Secondary Twinning to the Artificial and Natural Smoky Color

The twinned and untwinned areas of the quartz are found to differ markedly in their response to irradiation with x-rays. If whole wafers are bathed in x-rays the twinned bands are hardly tinted by the radia-

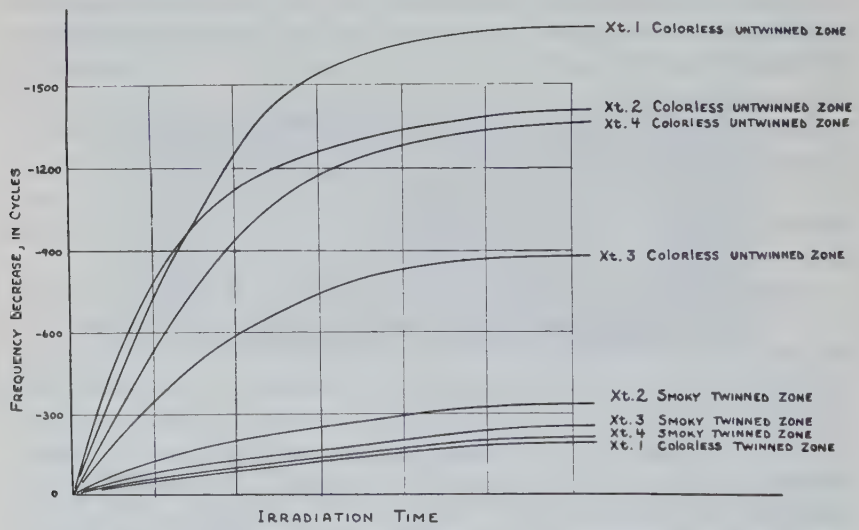

Fig. 6. Frequency change produced by irradiation of 8 mc. oscillator-plates cut from adjoining twinned and untwinned parts of single BT wafers.

tion while the adjacent untwinned quartz is relatively deeply colored. The arrangement of twin bands along growth zones in the quartz becomes apparent by the differential coloration of the zones produced in this way. The tendency to twin is thus associated with a variation in a quality of the quartz itself, this quality being zonally distributed in the crystal during its growth. A quantitative estimate of the variation in the response to radiation was obtained by fashioning 8 megacycle oscillator-plates from adjoining bands of twinned and untwinned quartz in single wafers. The plates were then irradiated and the resulting decrease in frequency[5] was measured and plotted against irradiation time (Fig. 6).

[5] Frondel, C., Effect of radiation on the elasticity of quartz: *Am. Mineral.*, **30**, 432–447 (1945).

The plates made from the twinned quartz exhibited extremely small frequency changes, comprising in fact the smallest responses yet noted in the study of irradiated oscillator-plates. The change in color is correspondingly weak. The plates cut from untwinned quartz, on the other hand, show changes roughly four to ten times as great. Even in the latter plates, however, the total change is only about the average, roughly 1400 cycles, obtained in ordinary BT plates of the same frequency. The

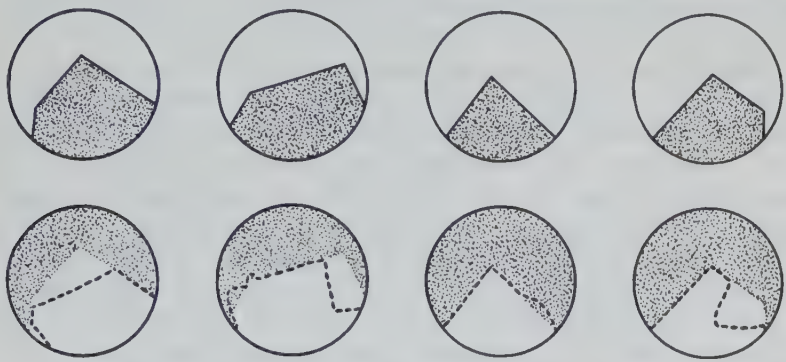

FIG. 7. The top row shows quartz discs cut across the coincident boundary of a natural Dauphiné twin and a natural smoky color zone. In the bottom row the same plates are shown after they have been baked at 650° C. and irradiated with x-rays. The artificial smoky color exactly marks the original twin boundary, but with the color intensities reversed, and the secondary twinning approximates the old boundary.

correlation between ease of secondary twinning by inversion or thermal shock and the tendency of the quartz to become colored by exposure to x-rays was first recognized by Zinserling,[6] who considered the weakly tinted quartz to be relatively pure and hence relatively plastic.

It is interesting to note that when areas of natural smoky color are present that they coincide with the weakly responsive, easily twinned quartz. Similarly, when quartz containing smoky zones, without twinning, is irradiated the lighter or colorless portions always are more deeply affected by the radiation.

A further relation between twinning and smoky color is sometimes noted in natural quartz crystals. Instances have been found in which the boundaries of natural Dauphiné growth twins coincide exactly with natural smoky color zones in the quartz. If the quartz is decolorized by baking at about 300° C. and is then irradiated, the two sides of the twin become differentially colored, but with the original lighter part now being the darker colored. The contrast is less marked if the original color is not first baked out. What is even more remarkable, it is found that when the crystal is detwinned by heating over 573° C. and is then cooled,

[6] See footnote 3.

the twinning formed on re-inversion follows closely or exactly the original twin boundary. Figure 7 (top row) shows a group of $\frac{1}{2}$-inch diameter discs about 0.012 inch thick cut normal to the Z = c-axis and containing coincident natural twin and smoky color boundaries. Figure 7 (bottom row) shows the discs after they have been heated to 650° C. and then irradiated with copper x-radiation. The secondary Dauphiné twinning follows approximately the original twin boundary, and the secondary smoky color follows exactly this boundary but with the relative intensity reversed from the natural relation.

The effect has so far been recognized only in a few specimens, in all of which the twin and natural color boundaries coincided. Twinned colorless or uniformly colored quartz does not seem to show the effect; but in these cases a possible differential response to radiation was not tested, and this may be the real criterion. Examples also have been found in which the parts of both Brazil and natural Dauphiné twins in colorless quartz respond unequally to radiation, but in these cases the behavior on baking was not investigated. Dauphiné twins produced artificially in originally untwinned quartz never are differentially colored by radiation. In the natural instances there seems to be a difference in some quality of the quartz across the original twin boundary that conditions the effect. It may also be noted in this connection that randomly selected colorless or uniformly tinted BT quartz plates when re-inverted at 573° C. are found, on a statistical basis, to be very much more disposed to secondary twinning when Dauphiné twinning is originally present than when absent,[7] although, as noted above, there is seemingly no tendency to exactly recapture the original twin boundaries.

Experiments with initially untwinned quartz of different degrees of smoky color reveals no correlation between the intensity of the natural color and the tendency to acquire secondary twinning by inversion. Groups of 10 to 30 plates were cut from each of several dozen raw crystals, baked simultaneously at 650° C., and then etched to reveal twinning. Separate colorless crystals from the same locality (Hot Springs, Arkansas) gave very different percentages of twinning and the same was observed of deep black smoky quartz. Rose quartz and citrine, however, were uniform in showing little or no inversion twinning.

The tendency to twin and the responsiveness to radiation may both depend upon a defect structure or impurity content of the quartz, the twinning being a reflection of an accompanying variation in the plasticity of the substance and the irradiation phenomena depending on the availability of traps for photoelectrons. The very small but apparently significant variations reported in the density, cell dimensions, rotatory power and indices of refraction of quartz are significant in this regard.

[7] Frondel, C., cited in footnote 3.

EFFECTS OF DIKES AND DISPLACEMENT MOVEMENTS ON SEDIMENTS IN CAPITAN QUADRANGLE, NEW MEXICO

RAYMOND SIDWELL,
Texas Technological College, Lubbock, Texas.

ABSTRACT

Mesozoic sediments of the Capitan quadrangle, central Lincoln County, New Mexico, were altered by intrusions of diorite and diorite porphyry dikes and by displacement movements along some of the dikes. The apparent effects of the two processes extend laterally about 30 feet on either side from the dikes in the sandstones and 20 feet in the limestones and shales. Some of the outstanding changes in the sediments include induration, a change in color, formation of workable beds of coal, replacement of carbonates, and a variation in the mineral content.

INTRODUCTION

The Capitan quadrangle, central Lincoln County, New Mexico, includes a portion of the Sacramento Mountains. The relief drops to lower levels except in a few isolated areas as the Capitan, Carrizo, and Sierra Blanco mountains. A network of dikes breaks through Mesozoic sedimentary rocks, and forms a conspicuous feature of the landscape.

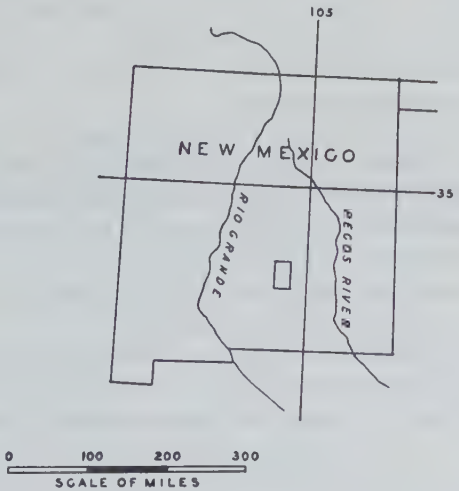

FIG. 1. Map of New Mexico showing the general position of Capitan quadrangle.

This paper deals chiefly with intrusions of diorite and diorite porphyry dikes. These constitute the larges individual intrusions of the area, some attaining a width of 200 feet. Their isolation in most of the quadrangle is sufficient to observe in detail the effects of the intrusions on the adjoining sediments. Although other types of dikes are present in the

Vera Cruz Mountains, they do not always contact directly the sedimentary materials.

Rocks in approximately 75 per cent of the dikes consist of a medium-grained diorite porphyry containing phenocrysts of plagioclase (Ab_9 An_1) feldspar. The core in the zoned plagioclase (about 10 per cent of the phenocrysts) is as basic as andesine (Ab_{65} An_{35}). Pericline in combination with albite twinning is well developed in all phenocrysts. Minerals comprising the ground mass are plagioclase (Ab_9 An_1) feldspar and mafic minerals: magnetite, olivine, and brown hornblende. The feldspar minerals in the ground mass are euhedral with a lath-like arrangement and have well developed pericline-albite twinning. Magnetite grains are small and some appear to be inclusions in olivine and hornblende. Olivine is represented by small euhedral grains that are equally distributed throughout the igneous mass. Mafic minerals constitute about half the ground mass.

Rocks in majority of the diorite dikes are medium to fine grained; a few are basaltic. The predominating black color so characteristic of these dikes is due to the abundance of magnetite and hornblende which overbalance the lighter colored feldspar minerals. Olivine, an abundant mineral, occurs as rounded crystals that are partially enclosed by magnetite and hornblende. Feldspar minerals with the exception of a decrease in plagioclase (Ab_9 An_1) are very similar to those in the ground mass of the diorite porphyry dikes.

Triassic, Jurassic, and Cretaceous sedimentary rocks are exposed in the quadrangle. Triassic sediments, probably the lower Dockum, consist of non-marine, yellow to gray crossbedded sandstones interlensed with thin layers of sandy shale. The Dockum is about 150 feet thick and crops out in the eastern and southeastern portion of the quadrangle. The mineral content in order of abundance is quartz, zircon, tourmaline, rutile, leucoxene, ilmenite, and magnetite.

Jurassic rocks, Morrison formation, are composed of vari-colored, crossbedded, non-marine sandstones and shales that attain a thickness of 125 feet. The Morrison sediments are exposed near the eastern margin of the quadrangle in east-facing escarpments. The minerals in order of abundance are quartz, tourmaline, hematite, magnetite, ilmenite, zircon, mica, leucoxene, and rutile.

The Cretaceous system is represented by the Dakota, Mancos, and Mesaverde formations. The Dakota formation is a compact, conglomeritic, gray, marine sandstone. It is approximately 60 feet thick and caps many of the east-facing escarpments. The minerals in order of abundance are quartz, mica, magnetite, tourmaline, zircon, epidote, and rutile.

The basal portion of the Mancos, the Greenhorn, is a dark compact, fossiliferous limestone. Above the limestone are calcareous shales, Carlile, which are about 140 feet thick and contain large septated concretions. Exposures of the Mancos are widely distributed in the central portion of the quadrangle. The heavy minerals are magnetite, ilmenite, hematite, tourmaline, zircon, and epidote.

The formations comprising the Mesaverde are probably equivalent to the Point Lookout and Menefee in the San Juan Basin, New Mexico

TABLE 1. MINERAL CONTENT OF UNALTERED DEPOSITS

Mineral	Dockum	Morrison	Dakota	Mancos	Point Lookout	Menefee
Magnetite	2.1	15.0	28.5	43.0	25.4	45.4
Ilmenite	2.7	12.1		17.5		
Tourmaline	25.9	21.4	15.6	11.4	21.9	9.2
Hematite	.8	18.1		17.5	31.9	
Epidote			5.2	2.6	1.4	6.5
Garnet					2.1	.9
Mica		9.1	41.5		7.5	
Zircon	44.9	12.1	6.6	8.0	9.8	38.0
Rutile	20.8	4.8	2.6			
Leucoxene	2.8	7.4				

(Reeside 1924). The Point Lookout attains a thickness of about 120 feet and consists of three compact sandstones separated by layers of yellow, sandy shale. The sediments are weakly calcareous and contain several fossil horizons. The heavy minerals consist of hematite, magnetite tourmaline, zircon, mica, garnet, and epidote.

The Menefee formation consists of carbonaceous shales and thin layers of dark brown sandstones. The shales are partially indurated and contain large ferruginous concretions. The heavy mineral content of the shales include magnetite, zircon, tourmaline, epidote, and garnet.

METHOD OF PROCEDURE

Field work involved two objectives: one was to note the visible effects of the intrusives on the adjoining sediments; the other was to collect specimens of igneous and sedimentary rocks for laboratory study. Thin sections of the igneous rocks were utilized to determine the mineral content and to classify the intrusions. Specimens of altered and unaltered sedimentary rocks were analyzed to secure the change in the carbonates and mineral content. The carbonates were digested with a weak solution of hydrochloric acid and are represented by the difference

in weight of the materials before and after acid treatment. Sedimentary materials were prepared for mineral analysis by the use of acid and by crushing to sand sizes with wooden blocks. After the minerals were separated into the light and heavy fractions by bromoform, the heavy minerals were divided into the magnetic and non-magnetic groups. Percentage composition of the minerals was secured by counting.

Changes in the Sediments

The sediments were altered by two processes: one (probably the more important) was by gases and heat associated with the intrusion; the second, by a displacing movement along some of the dikes. The combined effects of the two processes extended laterally about 30 feet from the dikes in sandstones and usually less than 20 feet in limestones and shales. Some of the changes in the sediments were apparent in the field but laboratory work was essential to reveal others.

Changes observed in the field. The chief visible modifications in sedimentary rocks involved induration, color changes, and coalification. The shales within three feet of the dikes were indurated to the extent of developing foliated characteristics. The color change in shales (with exception of the vari-colored Morrison sediments which developed a brick red) was from gray to almost black. The noticeable effects in sandstones extended four to six feet from the intrusions. These consist of the development of quartzitic characteristics and a change in color from gray to black. The darkening is especially apparent where basaltic dikes cut Dakota sandstone. Slicken-side materials, probably altered sandstones, were distributed throughout the area.

During deposition of the shales in Mesaverde, conditions in Capitan quadrangle favored extensive accumulation of carbonaceous materials. These materials when subjected to the combined effects of the intrusion and displacement movements produced a good grade of bituminous coal. The quality of the coal becomes increasingly inferior with increasing distance from the dikes.

Changes revealed by laboratory work. The principal changes in the sediments disclosed by laboratory work include replacement of carbonates and variation in mineral content. During the period of intrusion, the carbonates were partially and in some cases completely replaced in calcareous sediments and concentrated in the zone of contact. The amount of carbonates replaced varies with the distance from the dikes and the type of sediments. The carbonates in limestones and calcareous shales were modified about 20 feet laterally from the dikes, but complete displacement was limited to a rather narrow band extending less than four feet from the zone of contact. Calcareous sandstones of the area

are restricted to the upper Cretaceous, Point Lookout formation. The change of the carbonate content in sandstones (amounting to less than five per cent) was limited to a band four or five feet wide on either side of the intrusions. Carbonates are now concentrated as veins in the contact zone especially along dikes that break through carbonaceous shales. These veins are about one inch thick and are composed chiefly of transparent crystalline calcite.

The variation in mineral content of altered sediments when compared with that of the original deposits is brought about by the introduction of new minerals, and by a change of characteristics in original materials. Introduced minerals (magnetite, olivine, garnet, epidote, mica, and andalusite) apparently came from two sources: some are important constituents of igneous rocks and were probably derived from the intrusion, while others which occur along the zone of contact were quite likely formed during the process of metamorphism. The characteristics of detrital as well as introduced minerals have suffered discernible, alteration.

Magnetite is an important constituent of the original deposits but was probably also introduced into the altered sediments during the intrusion. This is evidenced by a substantial increase in the magnetite content. In addition, there are more conspicuous shiny black metallic grains with minute facets; an increase in the number of altered grains; and magnetite inclusions appear especially in the olivine.

Olivine is a rare mineral in unaltered sediments but becomes abundant in the intrusive rocks. Since the contact zone contains large quantities of olivine, it was very likely introduced by the intrusion. Its abundance in altered sediments ranges from 11 per cent of the heavy minerals in the shales to 17 per cent in sandstones. Detrital olivine consists of irregular fragments of which approximately 75 per cent have been partly altered to iron oxide and a fibrous material (probably serpentine).

Two varieties of garnet, andradite and almandite, are present in the zone of contact. Almandite consists of angular fragments that are characterized by being light pink in color, almost transparent, and by having rectangular surface markings. Andradite in well developed dodecahedrons is limited to the altered calcareous sediments. Garnets in the contact zone make up about three per cent of the heavy minerals in the shales and eight per cent in the sandstones.

The increase in the abundance of epidote in the contact zone suggests that some of the grains were formed during the process of metamorphism. Although epidote is widely distributed in the zone of contact, its maximum concentration appears in altered calcareous sediments.

Two types of mica, muscovite and a brownish-red variety, phlogopite,

are present in the altered sediments. As the latter variety is limited to the contact zone, it appears to be a product of metamorphism. It occurs chiefly as pseudo-hexagonal crystals that are almost opaque, and is concentrated in sediments that contain an abundance of iron-bearing minerals. Although muscovite is distributed throughout the contact zone, it is not concentrated in large quantities.

The only place where andalusite occurs is in the contact zone where it is found in well developed prismatic crystals and in greatly fractured grains. Andalusite constitutes less than four per cent of the heavy minerals in the shales and six per cent in the sandstones. Inclusions of carbonaceous materials usually as narrow bands parallel to the long axis of the mineral are common.

Other detrital minerals which are a part of the original deposits include quartz, tourmaline, and zircon. Of these, quartz has undergone apparent changes. It is represented as transparent fragments with conchoidal fracture and as reddish-brown, sub-rounded grains with a tendency toward elongation. Compared with the original deposits the principal changes are: numerous dark grains apparently resulting from impurities brought in by intrusives, the development of parallel lamellae (platy quartz) in about 10 per cent of the grains, and strain shadows and crenulated borders in many of the sub-rounded grains.

Summary

Sediments in Capitan quadrangle have been altered by the combined effects of the igneous intrusions and displacement movements adjacent to the dikes. Changes in these sediments involve: induration, color change, coalification of carbonaceous sediments, replacement of calcareous materials, introduction of new minerals, and a change in the characteristics of the original detrital minerals.

Reference

Reeside, J. B. Jr. (1924), Upper Cretaceous and Tertiary formations of western part of the San Juan Basin, Colorado and New Mexico: *U. S. G. S., Prof. Paper* **134,** p. 9.

A SECOND DISCOVERY OF INDERITE*

E. Wm. Heinrich

Abstract

A second occurrence of inderite ($Mg_2B_6O_{11} \cdot 15H_2O$), which was first described in 1937 by Boldyreva from the West Kazakstan, U.S.S.R., has been discovered. New chemical and powder x-ray data indicate the identity of the two materials. By Weissenberg x-ray methods the mineral is found to be triclinic with $a_0=8.14$ Å, $b_0=10.47$ Å, and $c_0=6.33$ Å. It has two good cleavages, a density of 1.860, hardness of 3, and is clear and colorless. The optical properties are: X=1.488, Y=1.508, Z=1.515, and 2V=63°.

Previous Work

Inderite was first named and described by A. M. Boldyreva (1937). It derives its name from the Inder borate deposits in West Kazakstan, Inder mountains, U.S.S.R. Until the discovery of the American material, the mineral had not been found elsewhere. In 1941 a specimen was submitted for identification by M. Vonsen of Petaluma, California, to the Harvard Mineralogical Laboratory where a complete investigation of the substance was undertaken.

Occurrence

In Russia, according to the published account, inderite is found at the Kzyl-tau deposit, West Kazakstan, where it occurs as small, white to pink, reniform nodules disseminated in a brick-red clay. The clay is composed of quartz, calcite and "hydrous basic magnesium carbonate." The only other borate present is hydroboracite which occurs in veinlets and lenses (Boldyreva, 1937). Information on the location and occurence of the American material has been withheld at the request of the discoverer.

Identification

The identification of the American mineral as inderite is based on four lines of evidence:

1. Identical chemical composition.
2. Partial similarity with published optical properties of the type material.
3. Similarity of x-ray powder data of the American material and that published for the type inderite.
4. Identity of the American mineral with artificially prepared inderite as shown by x-ray powder photographs.

X-Ray Investigation

No crystals of the mineral were discovered, but the specimen ex-

* Contribution from the Harvard Department of Mineralogy and Petrography, Harvard University, No. 272.

amined may be a fragment from a large single crystal. It is a tabular plate 3.5 cm. long, 2.5 cm. wide and 1 cm. thick. Two cleavages, making an angle of 66° 20′, are easily recognized. The intersection of these cleavages is parallel to the longest direction of the specimen.

X-ray rotation and Weissenberg photographs were taken on a cleavage fragment with the cleavage intersection as the axis of rotation. These photographs indicate a triclinic unit cell with the dimensions:

$$a_0 = 8.14\,\text{Å}, \quad b_0 = 10.47\,\text{Å}, \quad c_0 = 6.33\,\text{Å}.$$
$$\alpha = 96°56\tfrac{1}{2}', \quad \beta = 106°28', \quad \gamma = 106°03'.$$
$$\text{Axial ratio: } a_0:b_0:c_0 = 0.768:1:0.604.$$

The two cleavages become $b\{010\}$ and $\{1\bar{1}0\}$ and the rotation axis the $c[001]$ axis. The calculated volume of the unit cell is:

$$V_0 = a_0 b_0 c_0 \sin\alpha \sin\beta \sin\gamma^*$$
$$V_0 = 485.43\,\text{Å}^3.$$

With this value and the measured density (1.86), the molecular weight (M) of the unit cell is:

$$M = 547.28.$$

Physical Properties

One cleavage is perfect parallel to $b\{010\}$; the second is good parallel to $\{1\bar{1}0\}$. Cleavage faces have a vitreous to pearly luster; whereas the irregular surfaces have a dull, greasy appearance. The mineral is clear and colorless. The density is 1.860 (average of determinations on three different grains by the Berman microbalance). The hardness is 3; it is not scratched by calcite, nor does it scratch that mineral.

No cleavages are reported for the type inderite, which occurs as fine, prismatic needles in nodular aggregates. The hardness of the Russian mineral is stated to be less than 1, and the density is reported as 1.79. Because of the occurrence as aggregates of needles, a measurement of the density of the type material probably would result in a value lower than one obtained from determinations made on single crystal fragments which were without fractures or air spaces. Likewise, it is apparent that the true hardness of the original inderite was probably not measured and that only the separation of the small needles was observed.

Optical Properties

Orientation	n_{Na}		
X near b	1.488	± .002	Bx (−)
Y	1.508		2V = 63° ± 03°
Z∧c = −22°	1.515		$r > v$, weak

The optical data for the type inderite were listed as follows:

$N_g(nX?) = 1.488$
$N_m(nZ?) = 1.504$
2V large
Bx (−)
$Z \wedge c = 5°$

Boldyreva (1937) states, "No direct N_p (or nY?)measurements could be done, because the minute prisms lay down always almost with N_p vertical." Previously he states, "It is optically a biaxial, negative mineral, with a diffuse figure in convergent light and with a large 2V." These two statements are contradictory, for, if the slender prisms gave a negative biaxial figure from which 2V could be estimated, then from these needles only nZ and nY could be measured and not nX.

Chemistry

Table 1

	1	2	3	4	5	6		7
MgO	14.70	14.34	14.65	14.36	14.82	14.40	Mg	2.07
B_2O_3	36.41	35.60	36.20	37.31	36.69	37.32	B	5.95
H_2O	48.12	48.20	48.20	48.88	48.49	48.29	O	11.00
Rem.	0.86	2.62	0.97				H	30.40
Total	100.09	100.76	100.02	100.55	100.00	100.00	O of H_2O	15.20

1. Inderite from American locality; F. A. Gonyer, *analyst.*
   Remainder is: Insoluble 0.54, CaO 0.32.
2. Inderite from Inder Basin, U.S.S.R.; E. N. Egorova, *analyst*
3. Remainder for 2 is: SiO_2 0.71, Al_2O_3 0.10, Fe_2O_3 0.23, CaO 1.02, K_2O and N_2O 0.18, CO_2 0.38.
   Remainder for 3 is: SiO_2 0.13, Al_2O_3 0.02, Fe_2O_3 0.32, CaO 0.16, K_2O and Na_2O 0.17, CO_2 0.17.
4. Inderite, artificial; Feigelson, Grushvitsky, and Korobochkina (1939).
5. Analysis 1, recalculated to 100%.
6. Theoretical composition of $Mg_2B_6O_{11} \cdot 15H_2O$.
7. Atomic ratios of Analysis 1.

The new analysis approximates closely the formula $Mg_2B_6O_{11} \cdot 15H_2O$, which has already been proposed. The unit cell contains one formula weight of $Mg_2B_6O_{11} \cdot 15H_2O$. The calculated density agrees closely with the measured density:

$$d_{calc.} = 1.87$$
$$d_{meas.} = 1.86.$$

By means of the Law of Gladstone and Dale, it is possible to calculate approximately the mean index of refraction (n):

$$\frac{n-1}{\text{density}} = K$$

	p	k
MgO	14.82	.200
B_2O_3	36.69	.220
H_2O	48.49	.3355

The k values are from Larsen and Berman (1934).

$$\frac{n-1}{1.86} = K = .27304$$

$$n = 1.508.$$

This value compares favorably with the measured mean index of refraction, 1.504.

Inderite is easily soluble in warm dilute HCl. Before the blowpipe on charcoal it fuses at about 600°C. to an opaque white bead. Flame tests produce a very strong green flame of boron. Heated in the closed tube, inderite gives off large amounts of water with marked intumescence. The water gives a slight basic reaction.

Investigation by X-ray Powder Method

Boldyreva (1937) has given x-ray powder data for inderite and inyoite with iron radiation. Unfortunately, his method of presentation is somewhat ambiguous. He does not list the spacings (d) directly but tabulates the values $d\alpha/n$ with $n=2$ and α the α-wave length of iron radiation.

Feigelson, Grushvitsky and Korobochkina (1939) have synthesized inderite by using borax and magnesium sulfate heptahydrate in the proportions necessary to produce the substance. A water solution of these two salts was placed by them in a stoppered jar and kept at about 35°C. At the end of 24 days a crystalline precipitate had formed and was removed and analyzed (Table 1, 4). From this analysis and the optical properties, these authors were able to state, "that the salt obtained is a synthetic inderite."

Using the method outlined above, the author repeated the experiments and obtained a precipitate of rounded crystals at the end of three weeks.

X-ray powder photographs with iron radiation were taken of the American inderite and of the precipitate obtained by the Russian method. In Table 2 the results are given and compared with the data published by Boldyreva (1937).

TABLE 2. *X*-RAY POWDER DATA FOR INDERITE.
IRON RADIATION

	Inderite from America		Synthetic Inderite		Inderite from Inder Basin, U.S.S.R.	
	I	*d*	*I*	*d*	*I*	*d**
1	9	7.314	9	7.361		
2	5	5.955	5	5.923		
3	10	5.000	10	5.000		
4	3	4.235	2	4.230		
5	4	3.965	3	3.970	3	3.872
6	7	3.481	6	3.492	10	3.490
7	1	3.388	1	3.375	2	3.394
8	8	3.177	9	3.180	9	3.032
9	2	3.055	3	3.065	4	2.936
10	7	2.866	7	2.880	9	2.768
11	3	2.696	2	2.687	5	2.644
12	1	2.602	1	2.587	2	2.578
13	3	2.543	2	2.543	6	2.512
14	6	2.475	6	2.477	8	2.432
15	3	2.398	3	2.400		
16	3	2.280	3	2.282	4	2.214
17	2	2.095	1	2.096	3	2.060
18	4	1.963	6	1.965	2	2.014
19	1	1.927	1	1.925	2	1.968
20	2	1.872	2	1.873		
21	1	1.826	1	1.824		
22	2	1.782	2	1.780	2	1.756
23	3	1.739	3	1.739	7	1.736
24	1	1.662	1	1.659		
25	3	1.636	1	1.632	2	1.638
26	1	1.596	2	1.598	3	1.616
27	3	1.577	2	1.574		
28	2	1.538	2	1.539	5	1.542
29	1	1.504	1	1.491	2	1.504
30	1	1.473			3	1.458
31	2	1.421				
32	1	1.362				
33	1	1.345				
34	1	1.330				
35	1	1.293				
36	1	1.262				
37	1	1.219				
38	1	1.200				
39	1	1.175				
40	1	1.164				
41	1	1.155				
42	1	1.141				
43	1	1.069				
44	2	1.048				

* Recalculated from given values of $d\alpha/n$.

The identity of the inderite with the material synthesized is immediately apparent. The agreement with the reported spacings of the type material is not so complete, but the discrepancies must be ascribed to differences in measurement of the two films. It may be noted that values obtained for inyoite showed identical deviations from the *d* values for Russian inyoite.

Acknowledgments

It is the writer's pleasure to acknowledge the interest and assistance of Professor E. S. Larsen and the late Professor Harry Berman of Harvard University and Dr. C. Wroe Wolfe of Boston University.

References

1. Boldyreva, A. M. (1937), Investigation of inderite and the including rock: *Mem. Soc. Russe Min.*, ser. 2, **66**, 651–671 (Russian), 672 (English summary).
2. Feigelson, I. B., Grushvitsky, V. E., and Korobochkina, T. V. (1939), Synthesis of inderite: *C. R. (Doklady) Acad. Sci., U.R.S.S.*, **22**, 242–243.
3. Larsen, E. S., and Berman, H. (1934), The Microscopic Determination of the Nonopaque Minerals: *U. S. Geol. Survey, Bull.* **848**, 30–32.

NOTES AND NEWS

INCLUSIONS IN MUSCOVITE FROM MITCHELL CREEK MINE, UPSON COUNTY, GEORGIA

J. G. Lester, *Emory University, Georgia.*

The demand created by the exigencies of World War II for domestic mica suitable for industrial use stimulated the prospecting of new localities, the re-examination of old, abandoned properties, and the re-opening of mica mines which had been idle or semi-idle for several years. Many new and productive localities were found and mining instituted, while several of the older properties with a history of spasmodic mining were put back into steady production. As a result of these activities much excellent mica was mined in Georgia during the war years.[1]

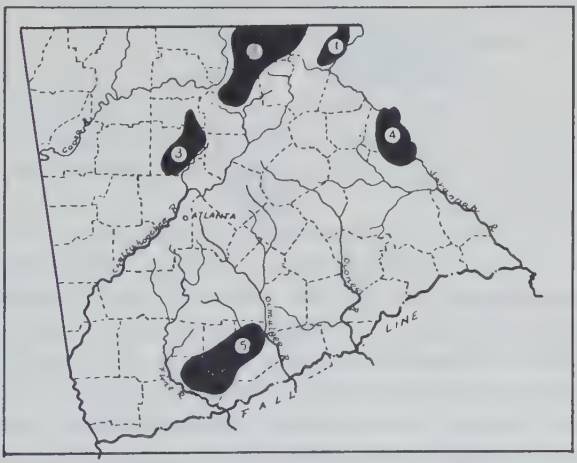

Fig. 1. Sketch map of Georgia north of the Fall Line showing location of mica zones. After Furcron & Teague, Bull. **48**, Georgia Geological Survey, 1943.

There are five mica-producing zones in Georgia. Zone No. 1 is located in the extreme north-eastern corner of the state in Rabun County; No. 2, the largest of the five zones, comprises parts of Towns, Union, Fanning, White, and Lumpkin Counties; No. 3 comprises parts of Pickens, Cherokee, and Fulton Counties; No. 4 lies in Hart and Elbert Counties along Savannah River; No. 5, the most productive and southernmost zone, comprises parts of Lamar, Monroe, Pike, and Upson Counties (see Fig. 1).

[1] Furcron, A. S., and Teague, K. H., Mica-bearing pegmatites of Georgia: *Georgia Geological Survey, Bull.* **48**, 18–19 (1943).

Mitchell Creek, one of the new mines, lies $7\frac{1}{2}$ miles southeast of Thomaston, Upson County, Georgia, and has been one of the more productive mines in Zone No. 5. The mica here occurs in a coarse pegmatite composed essentially of microcline, oligoclase, orthoclase, quartz, muscovite, and biotite. Accessory minerals are apatite, magnetite, and pyrite. Little or no alteration has taken place; all minerals appear fresh and clean.

The pegmatite cuts through a contorted augen gneiss of the Carolina series and generally is concordant with the gneissic structure, although occasionally apophyses of the pegmatite split around and across the gneissic bands. The vein trends about N 67° E and dips about 30° to the southeast. The dip, however, is highly variable and locally the contact between the gneiss and pegmatite is extremely indefinite. There is little, if any, banding in the pegmatite and, according to Maurice,[2] the Mitchell Creek pegmatite would correspond to a Class III pegmatite of the Spruce Pine, North Carolina, district.

The mica is hard, flat, ruby or rum-colored muscovite occurring in books which vary greatly in size. Some have been removed which weighed thirty to forty pounds and from which sheets as large as $6'' \times 6''$ were split. The average size of the books was such that sheets $2'' \times 2''$ could be obtained.

"A" structure and ribbon structure are occasionally seen in some of the smaller books or tablets. Spotty areas, resulting from included magnetite, apatite, or clay are the exception. Some tablets are wedge-shaped; a few are bent and contorted, but this is not common. All tablets apparently have developed a pseudo-hexagonal outline and exhibit greater translucency parallel to the cleavage than through the same thickness perpendicular thereto. Pale green to brownish-green colors are characteristic of the edgewise direction. Fairly good percussion figures are hard to obtain except on very thin sheets. Knotty cleavage is rarely encountered; thus splitting is relatively easy. On the other hand, small tablets of muscovite frequently interpenetrate one another or are included in larger tablets so that the cleavage planes are nearly at right angles, thus preventing or severely hindering splitting.

Biotite occurs in books varying in size from very small ($\frac{1}{8}''$ on a side) to large irregularly shaped books weighing several pounds. It is dark brown to nearly black, splits readily into thin sheets, and exhibits pleochrism from brownish green to dark brown. When viewed above a pinpoint light a poorly developed asterism may be noted. In contrast to the muscovite, however, almost perfect percussion figures can be developed

[2] Maurice, Chas. S., The pegmatites of Spruce Pine District, North Carolina: *Economic Geology*, **35**, No. 1, 57–67 (1940).

in fairly thick sheets with angles between percussion lines corresponding with those noted by Sterrett.[3]

Biotite and muscovite intergrowths, which are a unique characteristic of the Mitchell Creek pegmatite, may be classed in two groups or types. The first type is a tight intergrowth in which the two micas possess a common cleavage plane along which cleavage occurs without separation of the muscovite and the biotite. Thin sheets of this type, split with sharp needles, cleave as easily across the line of contact between the

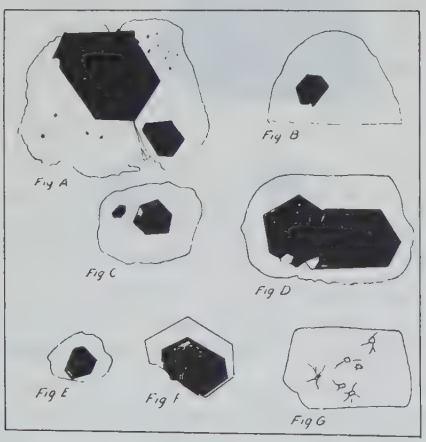

PLATE 1. Inclusions in muscovite. (Direct tracings made on light table, reduced $\frac{2}{3}$.)

two micas as within the individual crystal. Continued flexing of thin sheets, in which maximum flexure occurs along the line of contact or at right angles to the line of contact, also causes no noticeable separation of the two micas. Figures A, B, and H in Plates 1 and 2 illustrate this type of intergrowth.

The second type is a loose intergrowth in which the tablets of biotite and muscovite, though possessing common planes of cleavage, tend to separate when thin sheets are split across the line of contact. This is caused, in part at least, by the fact that the tablets of biotite, developed into strong pyramidal forms with pronounced eccentricity, are so arranged that each succeeding lower sheet of muscovite has a larger amount of biotite in it than the sheet above. Therefore it can slip more easily over the smaller part of the biotite pyramid. The axial convergence of the biotite pyramids is rapid and the corresponding variations in areas of cleavage surfaces are marked. Although the term

[3] Sterrett, Douglas B., Mica deposits of the United States: *U. S. Geological Survey, Bull.* **740,** 12, (1923).

pyramid is used to describe this type of intergrowth of biotite with muscovite, perhaps a more accurate term would be *frustrum of a pyramid* since no complete pyramid was observed. Figures C, D, E, F, J, and K in Plates 1 and 2 illustrate this type of intergrowth.

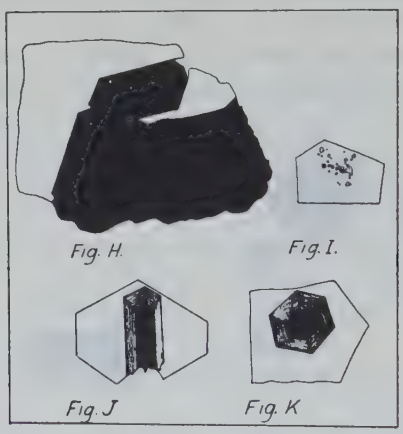

PLATE 2. Inclusions in muscovite. (Direct tracings made on light table, reduced $\frac{2}{3}$.)

The data in the following table will illustrate the eccentricity and the areal changes in the biotite pyramids of the second type:

Figure*	Thickness of sheet in mm.	Top area mm.^{2}	Bottom area mm.^{2}	Maximum axial convergence of pyramid faces
C	.75	64	198	73°
D (large)	2.51	592	788	40°
D (small)	2.51	326	756	44°
E	3.00	20	106	60°
K	3.50	141	396	60°

* These specimens were selected from several thousand as being representative.

Pale, greenish-yellow, euhedral crystals of fluor-apatite are frequently found embedded in tablets of muscovite. There is no uniformity of orientation; the *c*-axis of the apatite may lie parallel to the cleavage planes of the mica but more commonly cuts across them. Thus the two minerals do not possess a common cleavage plane. Even if the *c*-axis of the apatite happens to occur perpendicularly to the cleavage of the mica, thin cleavage sheets of mica from the tablets will not include thin layers of apatite. The apatite in some cases appears to have penetrated the

mica, and, in so doing, to have caused small ruptures which roughly resemble percussion cracks. In other cases, the time of crystallization of the two minerals was about the same, for thin folia of the mica penetrate shallowly into the apatite.

Often when an attempt is made to remove a crystal of apatite the folia of penetrating mica either bend or slip, causing the friable apatite to shatter. Or, if the mica is too tightly intergrown with the apatite to allow slippage, it remains as an unsightly fringe on the apatite prism. Some few apatite crystals of gem quality have been taken from the mine.

Microscopic inclusions of apatite prisms are common both in the muscovite and the biotite. In the biotite and muscovite intergrowths microscopic apatite crystals frequently lie so as to seem to penetrate both micas to the same depth.

Bright, brassy-yellow crystals of pyrite are frequently found as inclusions in the muscovite; with the exception of the biotite inclusions, they exhibit the most perfect coincidence in cleavage. Extremely thin sheets of muscovite split from a tablet will include pyrite of the same thinness. Appearing as crystals of a square or rectangular outline, a few show imperfectly developed striations when viewed by inclined light. Figure I of Plate 2 illustrates this type of inclusion.

Anhedral masses of milky or clear quartz are common inclusions in the larger tablets of muscovite. These do not extend all the way through the tablets but seem commonly to be localized near the center. No single large tablet (several pounds in weight) was completely discarded during splitting operations because of interference from quartz inclusions. Fracture lines in the muscovite caused by the quartz are similar to those caused by the apatite, but because the quartz crystallized much later than the muscovite there is no evidence of the two having common cleavage planes. Neither does there appear to be evidence of intergrowth between the quartz and muscovite.

Occasional small, light green euhedral crystals of microcline are included in the mica. Characteristically, upon exposure to sunlight, such crystals lose their green tint and assume a dead white color. The microcline, however, exhibits excellent cleavage and typical luster, but no specimen was found in which the feldspar and the mica possessed a common cleavage plane.

The muscovite at Mitchell Creek Mine is generally extremely hard, of excellent quality, uniform color, and normally almost flat. Although the owner, S. P. Cronheim, of Atlanta, Ga., has ceased operations, the deposit is, so far as can be judged without extensive subsurface prospecting, by no means exhausted.

A SIMPLE TEST FOR THE DETECTION OF THE BERYLLIUM MINERALS[1]

MARY H. FLETCHER[2] AND CHARLES E. WHITE[3]

The beryllium minerals in hand specimens are frequently confused with topaz, quartz, apatite, garnet and other minerals. A simple but specific qualitative chemical test for beryllium would preclude any uncertainty. This paper describes a rapid fluorescent microtest which can be used with assurance for the detection of this element. It is essentially an adaptation of the qualitative (1) and quantitative (2) procedures developed for the determination of beryllium.

The apparatus required consists of a platinum loop, several small pyrex test tubes, a porcelain spot plate (optional), and a source of ultra-violet light. The light source should preferably be a B-H-4 General Electric high-pressure mercury lamp equipped with a Corning Filter #5874. These lamps have a strong emission at 3654 Å and are excellent activators for the production of the fluorescence in the reaction involved here. However, lamps which produce light rich in 2537 Å radiation can be used. The fluorescence produced by the shorter wavelengths (2537 Å) is appreciably weaker than that induced by the longer wavelengths (3654 Å) consequently when such a lamp is used the solutions to be examined should be held about 2 inches from the light source.

The reagents required are:

Fusion mixture, (3:1) sodium carbonate+borax glass.
Hydrochloric acid, (1:1).
Sodium hydroxide, 10%.
1-4 dihydroxyanthraquinone (quinizarin), 0.03% concentration in *C.P.* acetone, kept in a glass-stoppered bottle;

or

1-amino-4-hydroxyanthraquinone, 0.03% concentration in *C.P.* acetone, kept in a glass-stoppered bottle.

(Dropping pipettes with rubber bulbs should not be used for either of the dye solutions, as acetone in contact with rubber reacts to form a brilliant blue fluorescent solution which ruins the test.)

The Test

Make a bead of the fusion mixture in the loop of a platinum wire in the usual manner. Add a single small crystal (about 40 mesh) of the

[1] Published by permission of the Director, Bureau of Mines, U. S. Department of the Interior.

[2] Chemist, Eastern Experiment Station, Bureau of Mines, College Park, Maryland.

[3] Chemist Consultant, Eastern Experiment Station, Bureau of Mines, College Park, Maryland.

mineral to be tested, or touch the bead to some of the powdered material. Heat again to decompose the sample. Dissolve the melt in 6–8 drops of (1:1) hydrochloric acid contained in a small test tube by placing the platinum wire and bead in the acid and warming. Cool the solution, and add 2 drops of either quinizarin or 1-amino-4-hydroxyanthraquinone. After addition of the dye, do not expose the solution to sunlight as strong light decomposes the dye and ruins the test. Add sodium hydroxide dropwise until the solution is purple. Avoid an excess, as this destroys the test. Expose the solution to ultra-violet light in a darkened room and examine for fluorescence. If beryllium is present a strong orange-red fluorescence (5700–6400 Å) is apparent.

The solution may be examined in the original test tube or it may be transferred into a non-fluorescent porcelain spot plate, or a drop of the solution may be placed on a piece of filter paper. The spot plate gives the clearest test.

If iron or manganese hydroxide precipitates upon addition of the sodium hydroxide, a condition which will occur if the mineral is helvite, the following procedure should be used.

Place a small amount (1–2 mg.) of the powdered material in a small test tube and boil with 6–8 drops of 1:1 hydrochloric acid. Make alkaline with an excess of sodium hydroxide. Filter the solution into a clean test tube, cool the solution and add 2 drops of either dye solution. Add hydrochloric acid dropwise until the purple color disappears and then sodium hydroxide until the solution is again purple. Examine for fluorescence as before.

Lithium when present in sufficient amounts will give the same reaction. However, if the small samples recommended are used, a negative test will be obtained with lithium-bearing minerals.

Acknowledgment

The study reported in this paper was under the general direction of J. B. Zadra, Chief, College Park Division, Metallurgical Branch, U. S. Bureau of Mines, and the immediate supervision of Alton Gabriel, and Morris Slavin. The writers are indebted to Alton Gabriel and Morris Slavin for comment and criticism.

References

1. White, C. E., and Lowe, C. S., *Ind. and Eng. Chem.*, **13**, 809 (1941).
2. Fletcher, M. H., White, C. E., and Sheftel, M. S., A fluorimetric method for the determination of beryllium in ores: *Ind. and Eng. Chem.*, anal. Ed., **18** [3], 1946.

THE CRYSTALLOGRAPHIC SOCIETY

The Crystallographic Society organized at Harvard University and Massachusetts Institute of Technology in 1939 is planning to resume its activities which were suspended during the war. The Society concerns itself with the science of crystallography, its applications to many fields such as Physics, Chemistry, Metallurgy, Ceramics and Biology, and is not restricted to the classical phases of crystallography commonly associated with mineralogy.

In 1940 this Society initiated the idea of launching a Journal of Crystallography. More recently, plans have been discussed by several Societies for starting a new international Journal of Crystallography to replace the *Zeitschrift für Kristallographie* which is no longer published. Since there is no other Journal devoted exclusively to crystallography, the Society takes an active interest in this new development.

A meeting to be held at Smith College is tentatively planned for March 21–23, 1946. Those wishing to present papers are requested to send title and brief abstract to Prof. M. J. Buerger, Mass. Inst. of Technology, Cambridge 39, Mass. The following invited papers have been arranged:

Prof. R. S. Bear, Massachusetts Institute of Technology, Long Spacings in Quasi-Crystalline Biological Preparations.

Prof. J. D. H. Donnay, Johns Hopkins University, The Lattice in Crystallography.

Mr. Howard T. Evans, Jr., Massachusetts Institute of Technology, Experimental Variation of the Habit of Sodium Nitrate Crystals.

Prof. I. Fankuchen, Brooklyn Polytechnic Institute, Crystallography, a Common Ground in Many Sciences.

Mr. Samuel G. Gordon, The Academy of Natural Sciences of Philadelphia, (Title to be announced).

Dr. Dan McLachlan, Jr., American Cyanamid Company, (Title to be announced).

Dr. N. W. Thibault, Norton Company, The Modifications of Silicon Carbide.

Dr. Edward Washken, Massachusetts Institute of Technology, Plastic Deformation and Recrystallization of Non-Metallic Crystals.

Dr. C. D. West, Polaroid Corporation, Crystals for Optical Polarizers.

Prof. Dorothy Wrinch, Smith College, Crystallographic Principles and Biological Problems.

All those wishing to renew membership or to become members of the Society or who desire further information, may write to William Parrish, Acting Secretary-Treasurer, The Crystallographic Society, Philips Laboratories, Inc., Box 39, Irvington, N. Y. Membership fees have been set at $1.00 for 1946. A new membership list will be compiled January 31, 1964.

A *Bulletin of the University of Utah*, vol. **34**, No. 15, Bibliography of the Geology and Mineral Resources of Utah, by Bronson F. Stringham, is now available and may be secured by writing the University Research Committee, University of Utah, Salt Lake City, Utah. The price is $1.00 per copy. In this bulletin the author has listed all articles and papers dealing with the geology, paleontology, mineralogy, and mineral resources of the state of Utah that have appeared to 1942 inclusive.

NEW MINERAL NAMES

Vernadite

A. G. Betekhtin, Genetic types of manganese deposits. *Bull. Acad. Sci. U.R.S.S., Sér. géol.*, **1944**, No. 4, 1–46. (Russian with English summary 43–46.)

The name vernadite is given, in honor of V. I. Vernadsky, to a mineral formed in the early stages of oxidation of manganese silicates and carbonates. The composition is stated to be $MnO_2 \cdot H_2O$, plus a varying amount of water. The mineral is widespread in occurrence and was previously taken to be manganite. It is black when massive, compact; reddish to chocolate brown when finely dispersed. Streak is chocolate brown.

Discussion. So vague a description scarcely warrants a new name.

Michael Fleischer

Christensenite

Tom. F. W. Barth and Aslak Kvalheim, Christensenite, a solid solution of nepheline in tridymite. *Norsk. Videnskaps-Akad. Oslo, Sci. Results Norwegian Antarctic Expeditions* 1927–1928, No. **22**, 1–9 (1944).

Tridymite from a lava on Deception Island has n (Na) $\alpha = 1.479$, $\beta = 1.480$, $\gamma = 1.483$, each about 0.01 higher than the corresponding n of pure tridymite. Spectrographic study showed the presence of Na, Al and traces of Fe and Ca. Quantitative photometric comparison with mixtures of quartz and nepheline showed that this tridymite contained 5.2% nepheline. Whereas normal tridymite has inversions at 117° and 163°, christensenite has a single inversion at 130° to 140°, the temperature varying somewhat for different crystals. It is probable that other tridymites from lavas will be found to belong to this series.

The name is for Consul Lars Christensen, who supported the expeditions financially.

M.F.

Unnamed

F. C. Partridge, Trevorite and a suggested new nickel-bearing silicate from Bon Accord, Sheba Siding, Barberton District. *Trans. Geol. Soc. S. Africa*, **46**, 119–126 (1943).

This is a preliminary description of a mineral associated with trevorite ($NiFe_2O_4$). It may be the nickel analogue of talc.

Chemical Properties: Analysis by H. J. Weall gave SiO_2 47.1, Al_2O_3, Cr_2O_3, TiO_2 none, Fe_2O_3 6.65, FeO 1.15, NiO 30.6, CoO 3.5, MgO 9.45, alkalies none, H_2O- 0.2, H_2O+ 1.45; sum 100.1%. This corresponds, after deduction of 5% trevorite, to $6NiO \cdot 3MgO \cdot 10SiO_2 \cdot H_2O$ or, as suggested in a note by J. E. de Villiers, to $(Ni,Mg,Fe,Co)_{14}Si_{16}O_{44}(OH)_4$. Talc is $Mg_{12}Si_{16}O_{40}(OH)_8$.

Physical Properties: Color is dark green in massive aggregates, apple-green in flakes. Streak, pale greenish white. Luster pearly in flakes, greasy to waxy in massive aggregates. H = 2–2½. G = 3.037. Cleavage micaceous, tough and flexible (like chlorites). Attracted in a strong field of an electromagnet, but not in a weak field.

Optical Properties: Biaxial negative, $n\mathrm{X} = 1.605 \pm .003$, $n\mathrm{Y} = n\mathrm{Z} = 1.650 \pm .002$, $2V_x = 14 \pm 2°$. Weakly pleochroic, Z = bluish green, X = yellowish green. Optic plane nearly normal to micaceous cleavage. Extinction is sensibly straight.

M.F.

NEW DATA

Ahlfeldite

ROBERTO HERZENBERG, Ahlfeldita, un nuevo mineral de Bolivia. Notas sobre la cobaltomenita. *Bol. Fac. Cienc. Exact. Fis Naturales, Univ. Córdoba (Argentina)* **VII,** No. 4, 4 pp. (1944).

Ahlfeldite was described in 1935 as an alteration product of penroseite (blockite) and was thought to be a nickel selenate. In 1937 it was stated to be identical with the cobalt selenate cobaltomenite. Re-examination of ahlfeldite shows it to consist of greenish crystals, probably triclinic, that contained much nickel and selenium, and little or no cobalt. The red color previously ascribed to the mineral is confined to a thin outer crust and may be due to native selenium. Ahlfeldite is therefore a valid species.

M.F.

At the December meeting of the New York Mineralogical Club held December 19, 1945 new membership and excursion committees were appointed and the Club voted to contribute to the Harry Berman Memorial Laboratory Fund. Mr. Clyde Schumacher of the Johns-Manville Co. spoke on the general subject "Asbestos."

Dr. George T. Faust, associate mineralogist of the U. S. Geological Survey has been appointed professor of mineralogy at Indiana University, and Dr. Eugene Callaghan, commodity geologist of the Survey, has been appointed professor of economic geology.